Supporting Information for:

Breaking bonds and breaking rules: inert-bond activation by $[(^{i}Pr_3P)Ni]_5H_4$ and catalytic stereospecific norbornene dimerization

Junyang Liu, Manar M. Shoshani, Kethya Sum, Samuel A. Johnson*

Department of Chemistry and Biochemistry, University of Windsor, Sunset Avenue 401, Windsor, ON, N9B 3P4, (Canada)

Fax: (+1) 519-973-7098

E-mail: sjohnson@uwindsor.ca

Experimental:

Unless otherwise stated, all reactions were carried out in an inert atmosphere under standard Schlenk or glovebox techniques. Benzene-d_6, toluene-d_8 and THF-d_8 were degassed by three freeze-pump-thaw cycles, and subsequently dried by running through a column of activated alumina. Dichloromethane-d_2 was degassed by three freeze-pump-thaw cycles and distilled from CaH_2. Anhydrous solvents and reagents were purchased from Millipore Aldrich (Sigma Aldrich), or Oakwood Chemicals. Cyclooctene and norbornene were distilled over Na under nitrogen prior to use. Trimethylsilyl chloride was distilled over CaH_2 prior to use. ^{1}H, $^{13}C\{^{1}H\}$, $^{19}F\{^{1}H\}$ and $^{31}P\{^{1}H\}$ NMR spectra were recorded on a Bruker AMX Spectrometer operating at either 300 MHz or 500 MHz with respect to proton nuclei. Hexamethyldisiloxane (HMDSO) was used as internal standard for kinetic studies.

The compounds $[Ni(^{i}Pr_3P)]_5H_6$, cyclooctyne, cis-1,2-bis(trimethylsilyl)ethene, 1,2-di(1-adamanyl)ethene, 1,2-di(1-adamantyl)ethyne and [SIPr]AuCl were synthesized according to literature procedures.[1-6]

Overview of attempts to synthesize 3 with a variety of alkenes and alkynes. Attempts were made to find a dihydrogen acceptor that would be reactive enough to form **3** from **1** at low temperatures, but that would resist further reactions with **3** to give carbide **2** or intermediates to **2** via C-H activation. It was thought that sterically protected alkenes or alkynes could be suitable, with perhaps alkynes being advantageous due to more rapid reactivity with **1**, allowing lower reaction temperatures to help stabilize **3**. Simple internal alkynes such as 3-hexyne were not useful; 3-hexyne was hydrogenated by $Ni(^{i}Pr_3P)]_5H_6$ and isomerized by chain-walking[7-12] to give the terminal alkene 1-hexene, which reacted rapidly with the in situ generated **3** to give carbide **2**, as shown in Scheme S1. Cyclic alkenes/alkynes or internal olefins with quaternary substituents were conceived as possible substrates. Unsaturated C=C bond sources such as cyclooctene, 1,2-bis(1-adamantyl)ethyne, and Z-bis(trimethylsilyl)ethene were screened. The reaction of **1** with 1,2-bis(1-adamantyl)ethyne proceeded slowly at room temperature and produced the expected

3 intermediate and both E- and Z-1,2-bis(1-adamantyl)ethane as products.[5] However, the production and decomposition of **3** reached a maximum after 5 min with only a maximum 20 % yield by ^{1}H NMR. In the case of Z-bis(trimethylsilyl)ethene, in addition to a small amount of **3**, E-bis(trimethylsilyl)ethene was also observed, likely due to insertion/β-H elimination. Both reactions did not go to completion even when unsaturated substrate were added in excess. Strained cyclic alkynes such as **4** were also considered as a strategy to improve the hydrogen accepting ability of the substrate, with the hypothesis that the ring strain released would provide a thermodynamic driving force for the cluster dehydrogenation step, allowing it to occur at low-temp while minimizing thermal decomposition of the resulting tetrahydride cluster, however, no more than 20 % conversion to **3** was achieved. It seemed likely that this was because the steric bulk used to stabilize the alkyne slowed its reaction with **1**; however, similar results were observed using the less sterically encumbered substrate cyclooctyne. It was noted that in high concentrations **3** rapidly decomposes back to **1** at room temperature, though not stoichiometrically, and without the loss of phosphine. Attempts to determine the reaction order of cyclooctene with **1** to give **3** gave no evidence that any change in reaction conditions could be used to render these alkynes and alkenes for the stoichiometric synthesis of **3**. For example, the addition of ^{i}Pr$_3$P was found to slow the decomposition of **3**, but similarly decreased the rate of its formation. A more reactive substrate proved necessary.

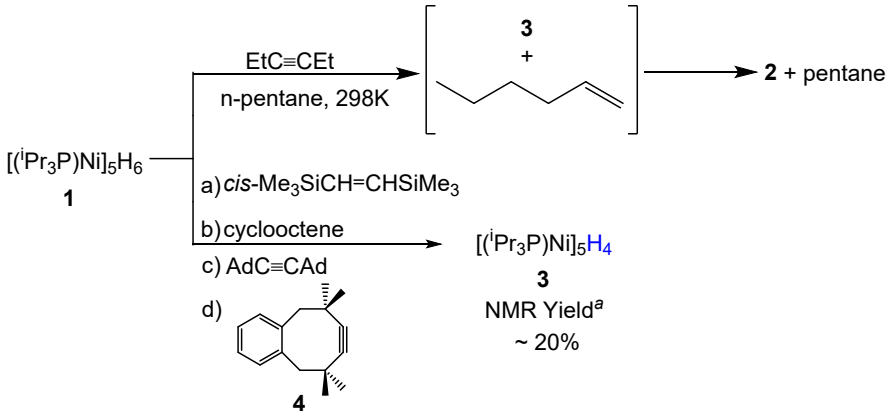

Scheme S1. Attempted synthesis of **3** using a variety of hydrogen acceptors. [a] ^{1}H NMR yield using hexamethyldisiloxane as an internal standard.

^{1}H NMR observation and characterization of [Ni(^{i}Pr$_3$P)]$_5$H$_4$ (3) from reaction of 1 with isobutylene. A solution of [Ni(^{i}Pr$_3$P)]$_5$H$_6$ （**1**） (27 mg, 0.025 mmol) in 0.6 mL of Benzene-d$_6$ was transferred to a J. Young. NMR tube which was subsequently connected to a Schlenk line. The solution is then put under three freeze-pump-thaw cycles and was exposed to 1 atm of isobutene added through the Schlenk line. The J. Young. NMR tube is then frozen with liquid nitrogen and allowed to warm up in the NMR probe. The reaction is monitored through ^{1}H NMR and resonances for isotopologues of **3** appear and disappear as the reaction proceeds. ^{1}H NMR (298 K, Benzene-d$_6$,

500 MHz): 3-d_0 δ 4.25 (septet, $^3J_{HH}$ = 7.1 Hz, 15H, P(C*H*(CH3)2), 3-d_1 δ 4.03 (septet, $^3J_{HH}$ = 7.1 Hz, 15H, P(C*H*(CH3)2), 3-d_2 δ 3.85 (septet, $^3J_{HH}$ = 7.1 Hz, 15H, P(C*H*(CH3)2), 3-d_3 δ 3.66 (septet, $^3J_{HH}$ = 7.1 Hz, 15H, P(C*H*(CH3)2), 3-d_4 δ 3.45 (septet, $^3J_{HH}$ = 7.1 Hz, 15H, P(C*H*(CH3)2).

Attempted synthesis of $[Ni(^iPr_3P)]_5H_4$ (3) using 1,2-Bis(1-adamantyl)ethyne. To a pre-cooled solution of **1** (20mg, 0.018 mmol) in *tert*-butyl methyl ether (0.4 mL) was added a cold solution (0.2 mL) of 1,2-Bis(1-adamantyl)ethyne (21 mg, 0.072 mmol) dropwise and mixed for 5 min. ^{1}H NMR initially show minimal presence of $[Ni(^iPr_3P)]_5H_4$ (3) and both E and Z isomer of 1,2-Bis(1-adamantyl)ethene indicated by their corresponding alkenyl C*H* resonances. Though the concentration of hydrogenation products continues to grow, the concentration 3 plateaus around 30% until starting to decrease.

Attempted synthesis of $[Ni(^iPr_3P)]_5H_4$ (3) using cis-Bis(trimethylsilyl)ethane. To a pre-cooled solution of 1 (20mg, 0.018 mmol) in *tert*-butyl methyl ether (0.4 mL) was added a cold solution (0.2 mL) of Z-Bis(trimethylsilyl)ethene (12 mg, 0.072 mmol) dropwise and mixed for 5 min. ^{1}H NMR initially show presence of $[Ni(^iPr_3P)]_5H_4$ and both trans and cis isomer of Bis(trimethylsilyl)ethene. The trans isomer is likely due to the catalytic isomerization of the cis-Bis(trimethylsilyl)ethene mediated by the cluster.

NMR scale synthesis of 3 with norbornene. In a J. Y. NMR tube was added a solution of **1** (20mg, 0.018 mmol) in *tert*-butyl methyl ether (tBuOMe)(400mg), it was frozen in liquid nitrogen evacuated for 5 minutes under high vacuum. Then another J. Y. tube containing norbornene (17 mg, 10 equiv., 0.18 mmol) in 200mg tBuOMe was vacuum transferred to the J. Y. tube with **1**. The sample was thawed briefly to allow thorough mixing of the content and then kept under liquid nitrogen until transferred to precooled NMR probe at 193 K. The reaction was allowed to warm up at 10 K increments until 283 K and reaction progress was monitored by ^{1}H NMR. It was observed that formation of **3** occurs at temperatures as low as 253 K, and the reaction was completed when warmed to 263 K, however, $[Ni(^iPr_3P)]_5H_4$ (**3**) also starts to decompose to form $[Ni(^iPr_3P)]_5H_6$ (**1**) at 263 K as indicated by the NMR spectrum showing ~96% conversion to **3** and only ~4% of **1** is present, all norbornene present were consumed.

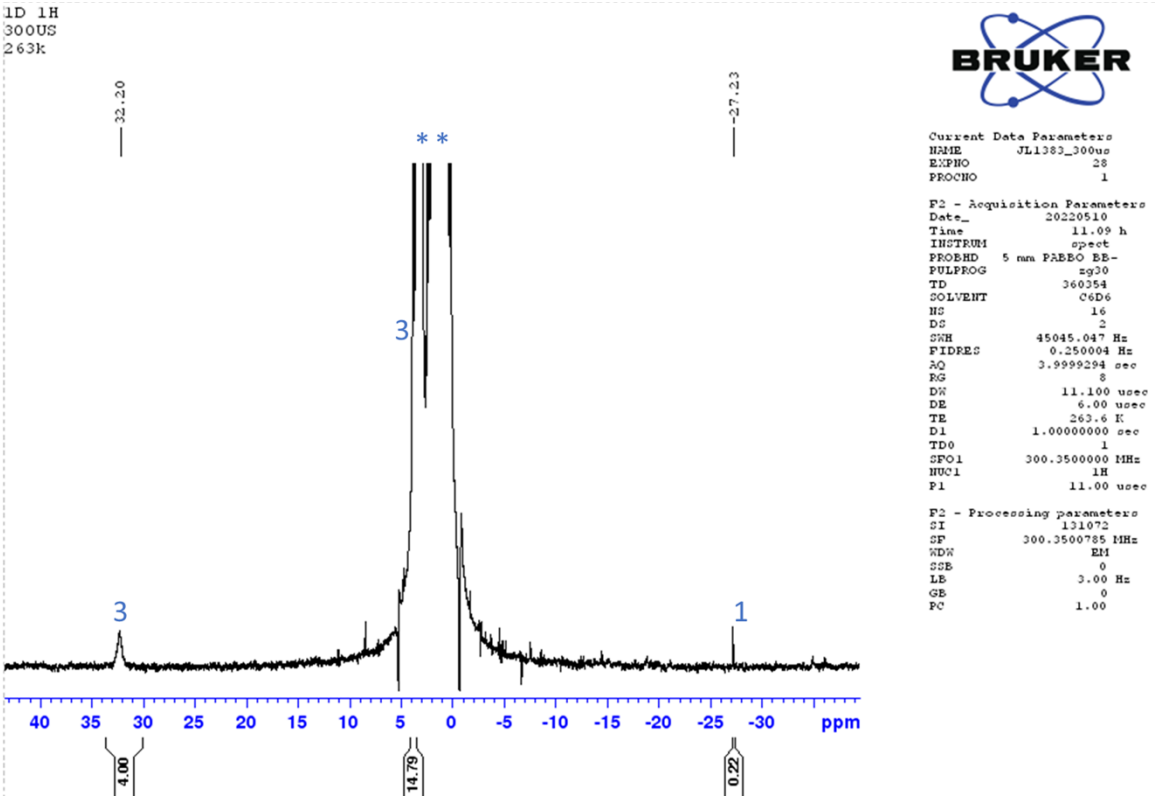

Figure S1. ^{1}H NMR spectrum showing 96 % conversion to **3** from **1** at 263 K. The hydride peaks of **3** and **1** are at δ 32.2 and -27.2, respectively. *Solvent signal: *tert*-butyl methyl ether.

Synthesis of [Ni(^{i}Pr$_3$P)]$_5$H$_4$ (3) using norbornene. To a n-pentane solution (10 mL) of [Ni(^{i}Pr$_3$P)]$_5$H$_6$ (1g, 0.91 mmol) pre-cooled to −20 °C in the glovebox, a cold n-pentane solution (10 mL) of norbornene (10 equiv.) was added dropwise while maintaining the overall reaction mixture below −10 °C. The mixture was mixed further for 10 min at −10 °C and the solution gradually turned dark burgundy in color. The mixture was pumped under vacuum to reduce solvent volume and was then left inside the glovebox freezer at −40 °C to recrystalize. Crystals suitable for X-Ray diffraction was grown from this solution over the course of 2 hrs. Yield: 398 mg (40%). The thermal instability of [Ni(^{i}Pr$_3$P)]$_5$H$_4$ in solution had made its handling extremely difficult, crystals of [Ni(^{i}Pr$_3$P)]$_5$H$_4$ dissolved in solution would rapidly form [Ni(^{i}Pr$_3$P)]$_5$H$_6$ and other unassignable complexes. ^{1}H NMR (THF-d$_8$, 253 K, 500 MHz): δ 1.37 (d, P(CH(*CH*$_3$)$_2$)$_3$, 90H, J = 6.6 Hz), 3.50 (sept, P*CH*,15H, J = 6.6 Hz), 25.24 (br s, Ni-*H*, 4H, $W_{1/2}$ = 112 Hz). ^{13}C{^{1}H} NMR (THF-d$_8$, 253 K, 125 MHz): δ 25.8 (s, P(CH(*CH*$_3$)$_2$)$_3$, 30C), 36.3 (s, P*CH*, 15C). ^{31}P{^{1}H} NMR (THF-d$_8$, 253 K, 202 MHz): δ399.6 (s, ^{i}Pr$_3$*P*). Calculated elemental analysis: C: 49.19; H: 10.00; N: 0.00 Found: C: 48.95; H:9.86; N: 0.00.

Due to the thermal instability of **3**, solutions sufficiently concentrated to give sufficient signal to noise for multinuclear NMR spectra invariably show some conversion back to **1**.

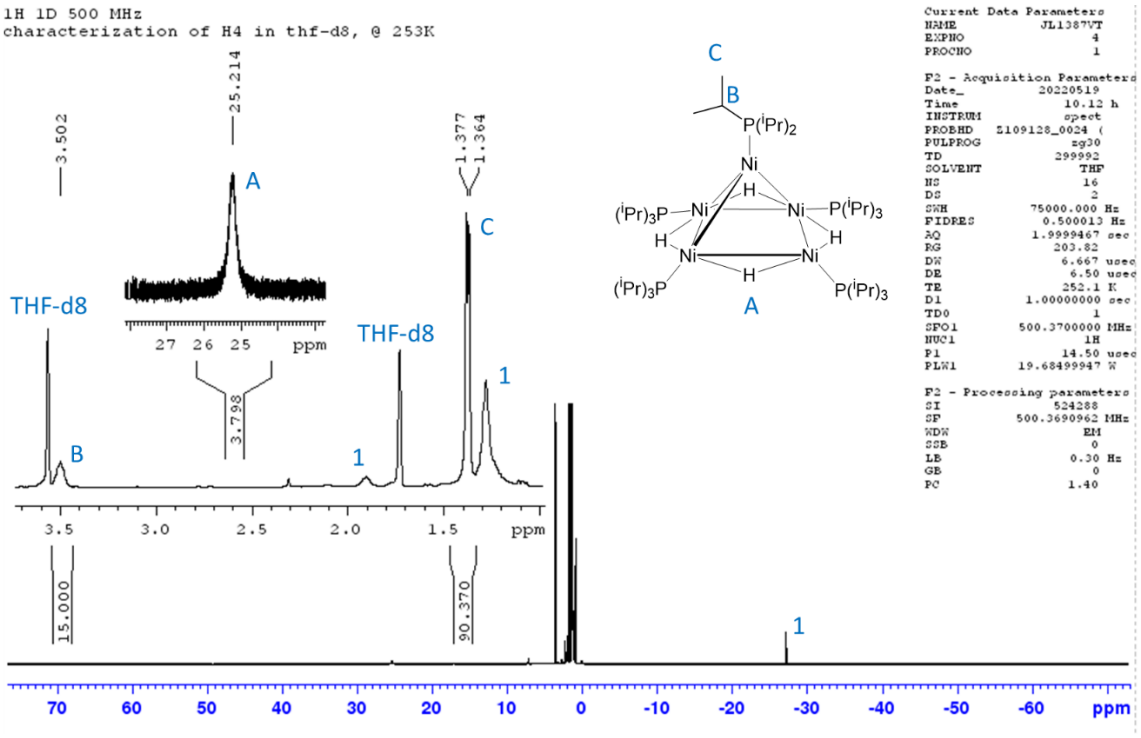

Figure S2. ^{1}H NMR spectrum of **3** in THF-d_8 at 253 K.

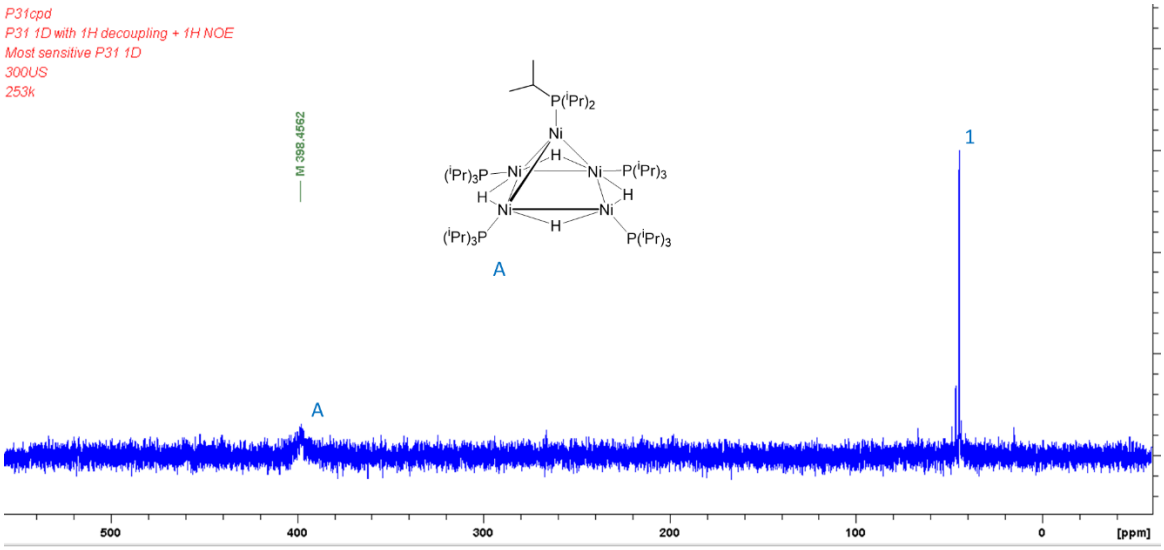

Figure S3. ^{31}P{^{1}H} NMR spectrum of **3** in THF-d_8 at 253 K.

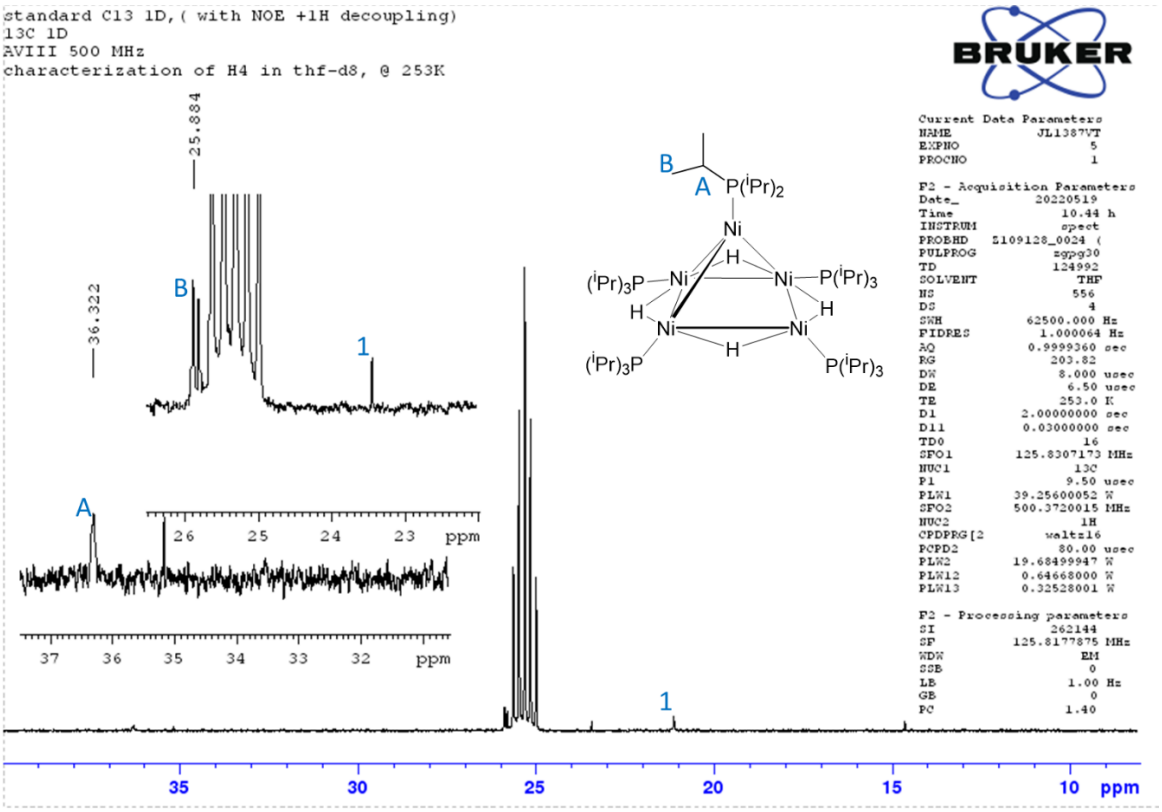

Figure S4. $^{13}C\{^{1}H\}$ NMR spectrum of **3** in THF-d_8 at 253 K.

Variable-temperature NMR of 3 in THF-d_8. A sample of **3** (20mg, 0.018 mmol) was dissolved in a pre-cooled THF-d_8 at -40 °C, and the sample was quickly transferred to an NMR tube and cooled in a −78 °C bath prior to analysis in an NMR probe at 193 K to minimize temperature fluctuations. The ^{1}H and $^{31}P\{^{1}H\}$ NMR spectra were recorded between 193 K to 293 K, and the $^{13}C\{^{1}H\}$ spectra were recorded between 253 K to 283 K.

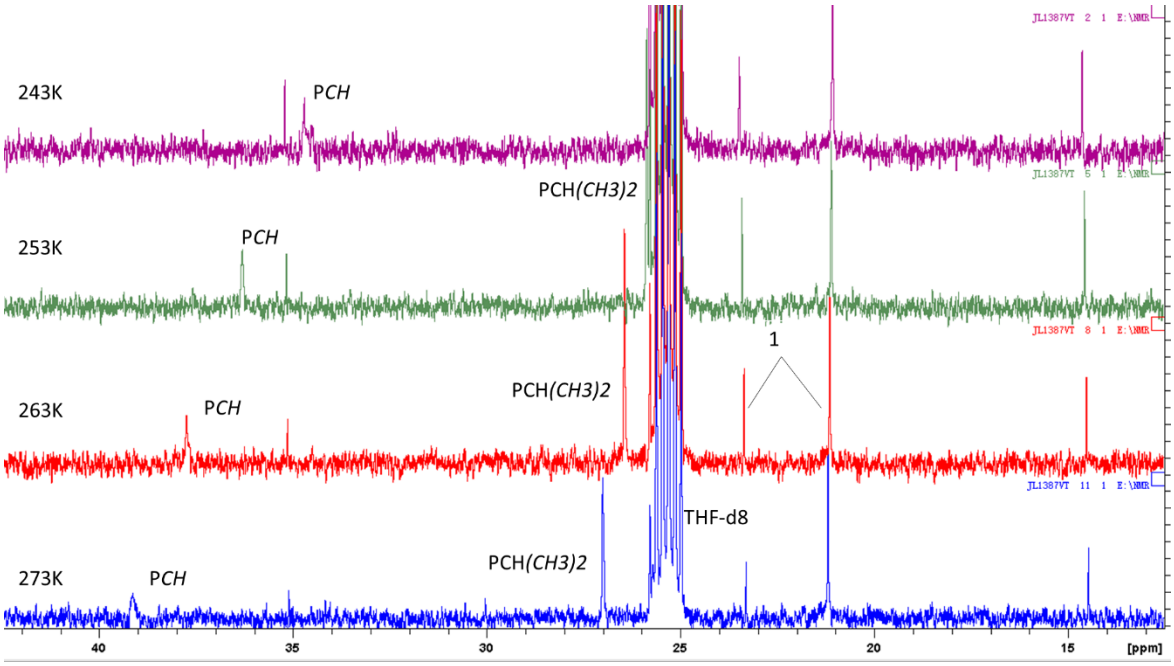

Figure S5. Variable-temperature $^{13}C\{^{1}H\}$ NMR spectrum showing the temperature dependence of carbon shifts of **3** in THF-d_8 from 243 to 273 K.

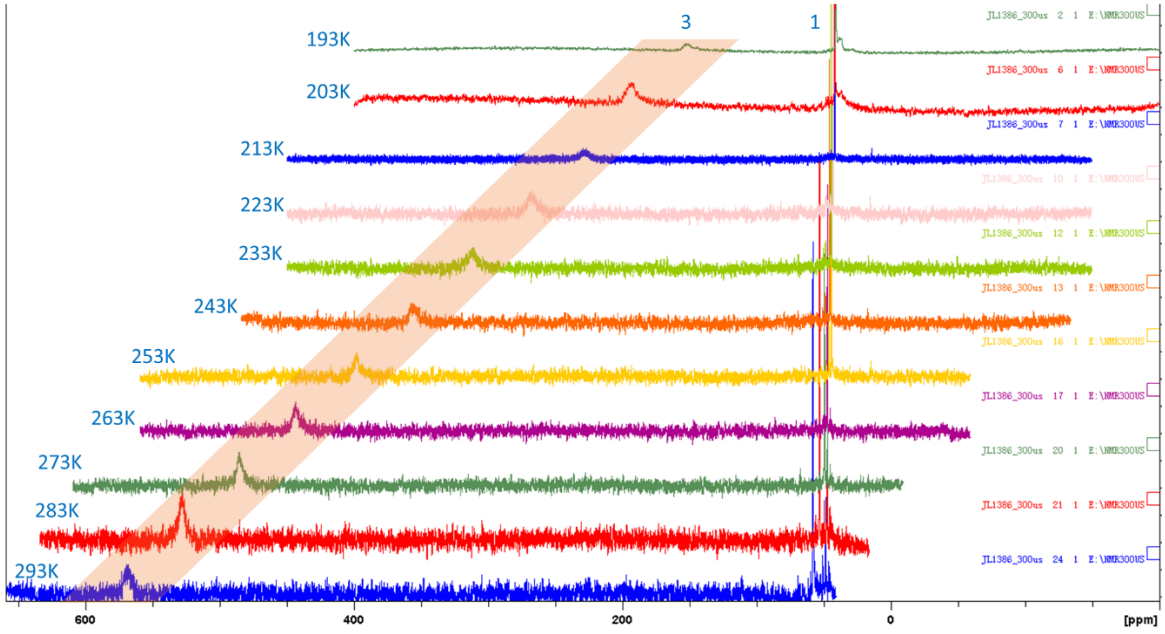

Figure S6. Variable-temperature $^{31}P\{^{1}H\}$ NMR spectrum showing the temperature dependence of phosphorus shifts of **3** in THF-d_8 from 193 to 293 K.

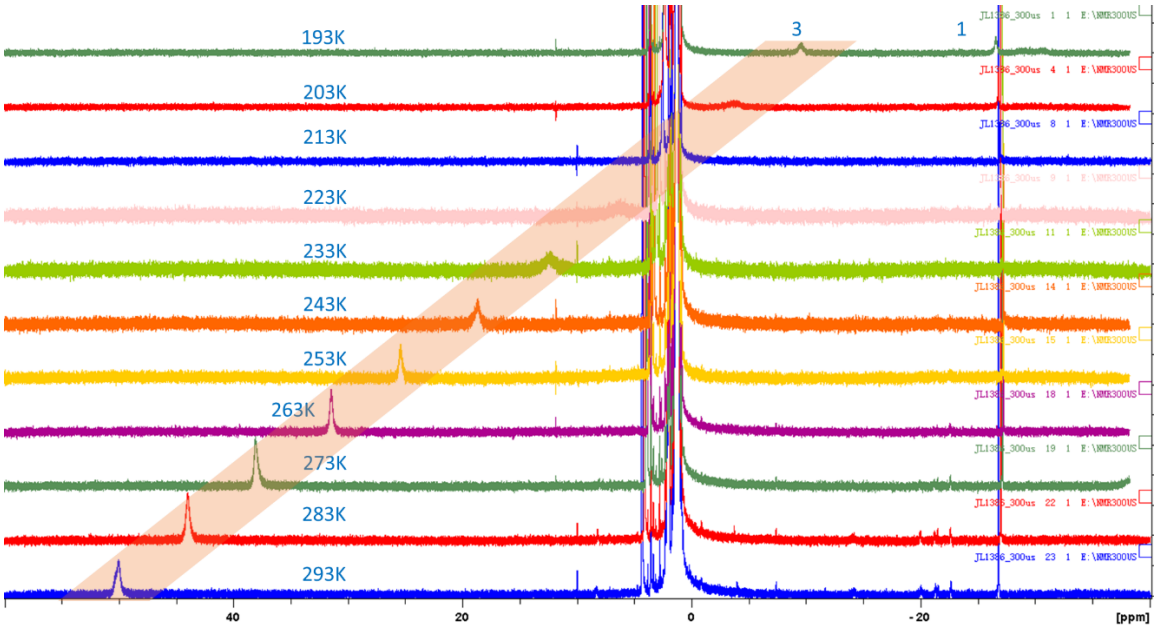

Figure S7. Variable-temperature ^{1}H NMR spectrum showing the temperature dependence of hydride shifts of **3** in THF-d_8 from 193 to 293 K.

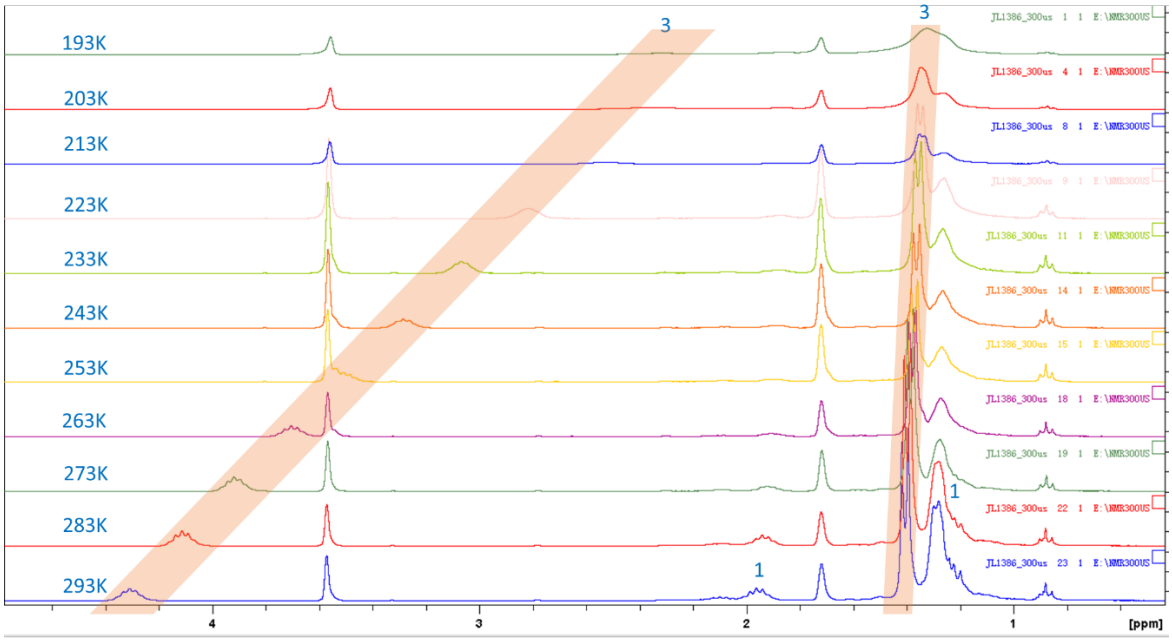

Figure S8. Variable-temperature ^{1}H NMR spectrum showing the temperature dependence of PC*H* and PCH(CH_3)$_2$ shifts of **3** in THF-d_8 from 193 to 293 K.

Catalytic dimerization of norbornene. To a solution of **1** (5 mol%) in n-pentane (5 mL) pre-cooled below −20 °C, a solution of norbornene (171 mg, 1.81 mmol) in n-pentane (2 mL) was added dropwise while stirring. The mixture was stirred for 10 min to ensure the completion of reaction,

then solvent was removed under vacuum and the solid residue was dissolved in undried hexanes and filtered through a short silica column. The column was rinsed with hexanes and combined with all organic washings. Dried with $MgSO_4$ and volatiles removed under vacuum to give a single isomer of norbornene dimer as a clear oil (101 mg, 59 %). ^{1}H NMR ($CDCl_3$, 298 K, 500 MHz): δ 1.16-1.32 (m, 8H), 1.56-1.59 (m, 6H), 1.95 (s, 1H), 1.98 (s, 1H), 2.33 (m, 2H), 2.78 (m, 2H). ^{13}C{^{1}H} NMR ($CDCl_3$, 298 K, 125 MHz): δ 28.81, 29.92, 36.85, 37.20, 40.05, 41.96, 132.11.

NMR scale catalytic dimerization of norbornene to rule out 1 as the active catalyst. To a Teflon cap sealed J. Young NMR tube was added freshly prepared **1** (20 mg, 16 mol %) in a N_2 atmosphere glovebox. The tube was sealed, removed from the glove box and attached to a Schlenk line. The tube was then cooled in liquid nitrogen. A *tert*-butyl methyl ether solution (0.5 mL) containing 0.02 M of hexamethyldisiloxane as an internal standard and norbornene (10 mg, 6 equiv) was vacuum transferred to the J. Young NMR tube. The contents were warmed slightly to dissolve **3**. The tube was transferred to an NMR spectrometer precooled to 193 K. The probe was warmed to 253 K and the reaction was monitored by ^{1}H NMR. Cluster **1** was completely consumed within minutes of warming, with a significant amount of norbornane formed. At this point, norbornane is the major organic product, and the dimerization product was present at ½ the norbornane concentration. Unreacted norbornene remained. After the disappearance of **1**, the dimerization product is seen to grow with respect to the norbornane peak, until no norbornene remained. No additional norbornane was formed after the disappearance of **1**, by integration with respect to the internal standard. This experiment rules out **1** as the active dimerization catalyst.

Synthesis of [(SIPr)Au(η^2-(Z) anti-(bis-2,2'-norbornylidene))]$^+$[SbF6]$^-$ [SIPr]AuCl (165 mg, 0.26 mmol) and $AgSbF_6$ (91 mg, 0.26 mmol) were mixed in 3 mL of dry DCM at 0 °C under nitrogen for 5 min, a solution of the (Z) anti-(bis-2,2'-norbornylidene) (55 mg, 0.29 mmol) dissolved in 1 mL of dry DCM was added dropwise, and the reaction mixture was stirred overnight at room temperature. The mixture was filtered through Celite and the solvent volume was reduced to 1 mL and an excess amount of hexane (ca. 5 mL) was added to cause the precipitation of the product as white powder (190 mg, 71 %). ^{1}H NMR (CD_2Cl_2, 298 K, 500 MHz): δ 0.51 (m, 1H), 0.54(m, 1H), 0.65 (m, 1H), 0.99-1.05 (overlapping m, 4H), 1.14 (m, 1H), 1.29 (overlapping m, 1H), 1.38 (d, 12H, J = 6.4Hz), 1.39 (d, 6H, J=6.7Hz), 1.40 (d, 6H, J=6.7Hz), 1.50 (m, 1H), 1.625 (m, 2H), 1.73 (dd, 1H, J=16Hz, 2Hz), 2.02 (m, 2H), 2.09 (m, 1H), 2.33 (m, 1H), 2.56 (d, 1H, J=4Hz), 2.58 (d, 1H, J=3.6Hz), 3.03 (sept, 2H, J=6.7 Hz), 3.08 (sept, 2H, J = 6.7Hz), 4.28 (m, 4H), 7.34 (dd, 2H, J=4.4 Hz, 1.4Hz), 7.36 (dd, 2H, J=4.4 Hz, 1.4Hz), 7.52 (t, 2H, J=7.8Hz). ^{13}C{^{1}H} NMR (CD_2Cl_2, 298 K, 125 MHz): δ 23.8, 24.4, 24.5, 25.1, 27.4, 27.5, 28.3, 28.9, 29.0, 29.2, 35.8, 36.8, 39.4, 39.5, 40.0, 41.9, 45.3, 45.7, 125.1, 125.2, 130.6, 131.6, 133.5, 133.8, 146.6, 146.6, 199.9. ^{19}F{^{1}H} NMR (CD_2Cl_2, 298 K, 470 MHz): δ – 124.2 (6F, overlapping 1:1:1:1:1:1:1:1 octet and 1:1:1:1:1:1 sextet due to ^{121}Sb and ^{123}Sb).

X-ray Crystal Structure of [(SIPr)Au(η^2-(Z) anti-(bis-2,2'-norbornylidene))]$^+$[SbF6]$^-$. Crystals suitable for X-ray diffraction were grown by the slow diffusion of hexane into a DCM solution of the product. The largest residual density Q peak is within 0.7 Å of Au(1). All the largest residual density Q peaks encircle the Au(1) atom and are not indicative any obvious disorder or error.

Source of isotope shifts for deuterated isotopologues: Shifts like those reported here for species that have thermally accessible paramagnetic states are well-documented; a brief description of their cause is provided as an aid to the reader. The difference in vibrations between hydrogen and deuterium leads to a slight difference in element-H versus element-D bond lengths, with the element-D bonds being slightly shorter. For C-H vs C-D bonds the difference is ~0.005 Å. In this way, hydride and deuterides are every so slightly electronically different ligands. In complex **3** each replacement of Ni-H by Ni-D causes the triplet state to lie slightly higher in E compared to the singlet state (modeled as a difference in the singlet-triplet gap of ~0.07 kcal.mol^{-1} for each D, as shown below). The higher energy of the triplet state means it will have a lower Boltzmann population, and thus the shift from the expected diamagnetic value of the singlet state will decrease for each hydrogen exchanged with deuterium.

Modeling the temperature dependent $^{31}P\{^{1}H\}$ shift of 3 and its deuterated isotopologues. The ^{31}P NMR chemical shift of **3** and its isotopologues were fit to a formula describing the shift as arising from the population of an excited triplet state, where the excited triplet state affects the chemical shift by a Fermi contact shift with a with T^{-1} dependence and a pseudocontact (dipolar shift) with a T^{-2} temperature dependence at the high-temperature limit. Attempts to improve the model by adding additional parameters, such as allowing additional T–3 and T–4 terms to fit the dipolar shift did not significantly influence the model. The fit was obtained by a least squares minimization of the differences between observed and modelled shifts using the Solver function in Microsoft Excel. The following equations summarize the model used:

$$\Delta G = \Delta H - T\Delta S + n\Delta D \quad (1)$$

$$p_{triplet}(T) = \frac{3e^{-\frac{\Delta G}{RT}}}{1 + 3e^{-\frac{\Delta G}{RT}}} \quad (2)$$

$$p_{singlet}(T) = 1 - p_{triplet}(T) \quad (3)$$

$$\delta_{model} = p_{singlet}(T) \times \delta_{singlet} + p_{triplet}(T) \times \left(\frac{C_1}{T} + \frac{C_2}{T^2} + \delta_{triplet}\right) \quad (4)$$

$\Delta G = Gibbs\ free\ energy\ of\ excited\ triplet\ state\ relative\ to\ ground\ singlet\ state$

$\Delta H = Enthalpy\ of\ excited\ triplet\ state\ relative\ to\ ground\ singlet\ state\ for\ 3$

$T = temperature\ in\ Kelvin$

$\Delta S = entropy\ of\ excited\ triplet\ state\ relative\ to\ ground\ singlet\ state\ for\ 3$

$n = number\ of\ deuterium\ in\ isotopologue$

$\Delta D = singlet\ to\ triplet\ energy\ \ change\ from\ replacement\ of\ H\ ligand\ by\ deuterium$

$p_{triplet}(T) = fraction\ in\ triplet\ state\ at\ temperature\ T$

$p_{singlet}(T) = fraction\ in\ singlet\ state\ at\ temperature\ T$

$\delta_{model} = modeled\ ^{31}P\ NMR\ chemical\ \ shift\ in\ ppm$

$\delta_{singlet} = chemical\ shift\ of\ singlet\ state\ 3$

$C_1 = coefficient\ for\ Fermi\ Contact\ shift$

$C_2 = coefficient\ for\ pseudocontact\ (dipolar)\ shift$

$\delta_{triplet} = chemical\ shift\ of triplet\ state\ of\ 3\ without\ contact\ and\ pseudocontact\ terms$

The final model was simplified by assuming $\delta_{triplet} \cong \delta_{singlet}$and instead of optimizing ΔS, it was estimated as Rln(3), due to the triplet spin degeneracy of the excited triplet state. This left 5 variables to be optimized. The model and parameters are given in Figure S9.

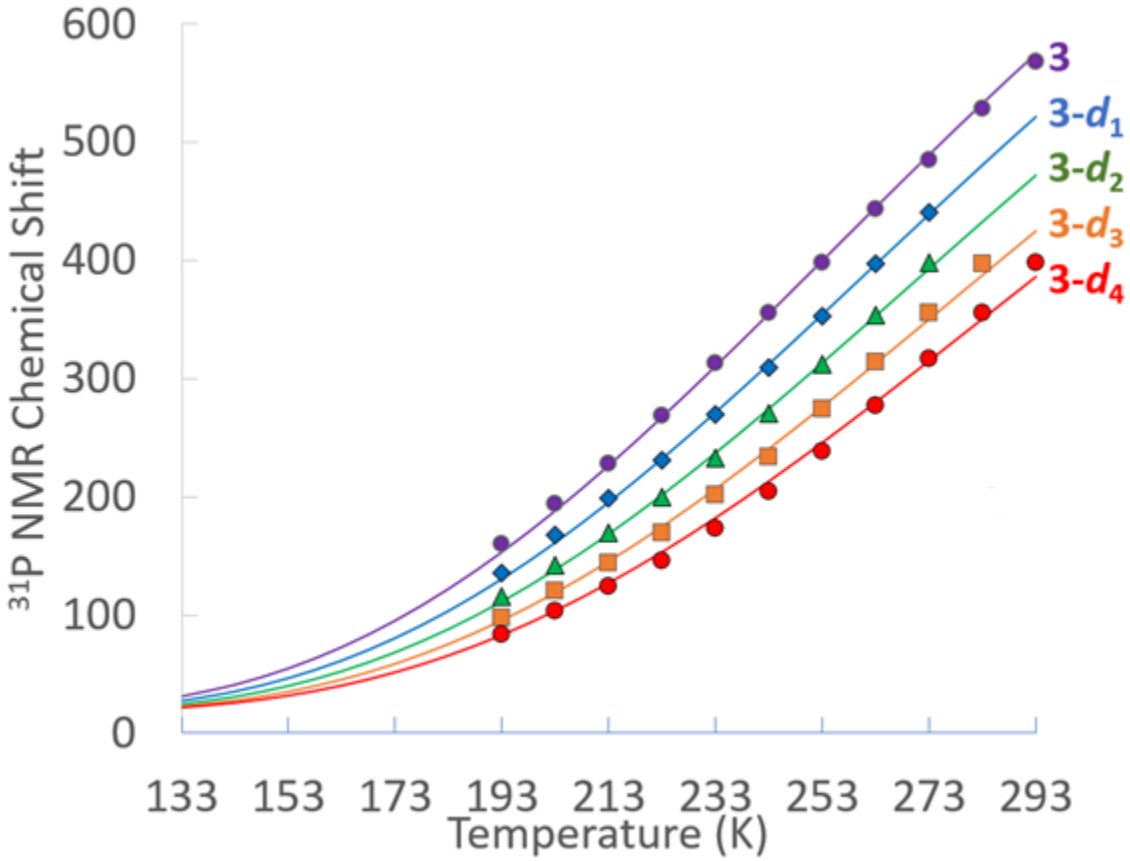

Figure S9. The temperature dependence of the $^{31}P\{^{1}H\}$ chemical shifts of **3** in THF-d_8 (purple circles) and the **3-*d*$_1$** (blue diamonds), **3-*d*$_2$** (green triangles), **3-*d*$_3$** (orange squares) and **3-*d*$_4$** (red circles) isotopologues in toluene-d_8. The solid lines show a fit based on the Boltzmann population of a low-lying triplet state. Here ΔH, ΔD, $\delta_{singlet}$, C_1 and C_2 were optimized and ΔS was set at Rln3. Optimized parameters: $\Delta H = 2.14\ kcal \cdot mol^{-1}$, $\Delta D = \ 0.07075\ kcal \cdot mol^{-1}$, $\delta_{singlet}$= 16.3 ppm, $C_1 = \ 1.03 \times 10^6$, C_2 ==– 4.30×10^7.

Modifying the model to include higher order T^{-3} or T^{-4} dipolar terms provided minimal improvement to the model. Similarly, excluding the pseudocontact term ($C_2 = 0$) generated a reasonable fit, shown below in Figure S10. The value of ΔH was not greatly affected between models. For example, setting the $\delta_{singlet}$ to a more reasonable value of 40.0 ppm changed ΔH by only 0.14 $kcal \cdot mol^{-1}$ after least squares minimization. Further improvements to the equation could be made by assuming a temperature dependence on ΔD, which is reasonable given its fundamental cause is vibrational differences between the hydride and deuteride, though such additional parameterization is unlikely to significantly change the estimated value of ΔH.

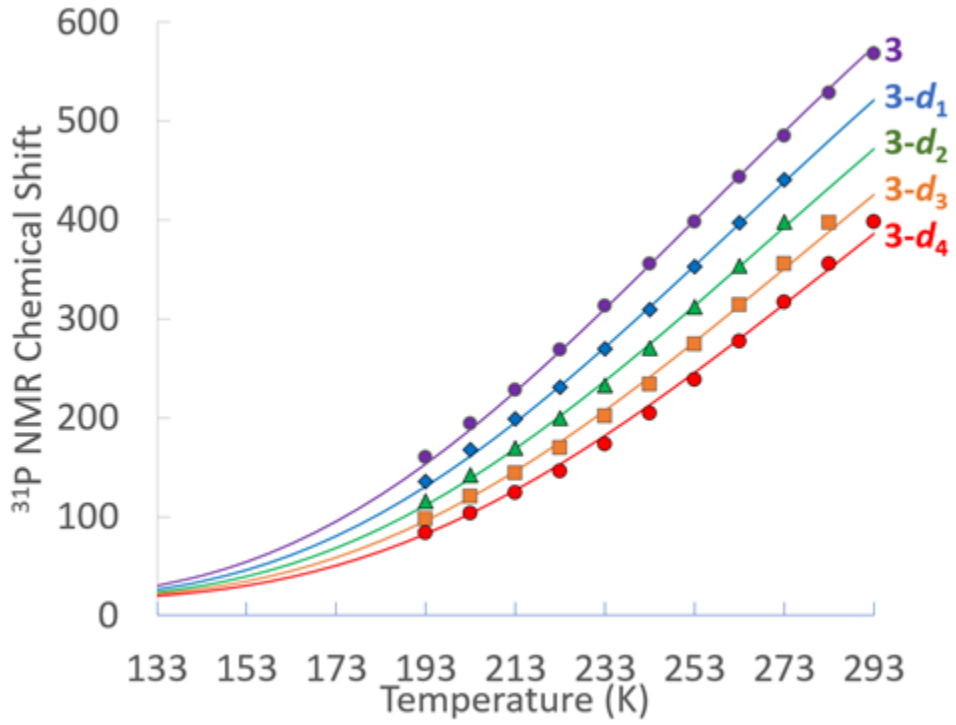

Figure S10. The temperature dependence of the $^{31}P\{^{1}H\}$ chemical shifts of **3** in THF-d_8 (purple circles) and the **3-*d*$_1$** (blue diamonds), **3-*d*$_2$** (green triangles), **3-*d*$_3$** (orange squares) and **3-*d*$_4$** (red

circles) isotopologues in toluene-d_8. The solid lines show a fit based on the Boltzmann population of a low-lying triplet state. Here ΔH, ΔD, δsinglet and C_1 were optimized and ΔS was set at Rln3. Optimized parameters: $\Delta H = 2.21\ kcal \cdot mol^{-1}$, $\Delta D = \ 0.06949\ kcal \cdot mol^{-1}$, $\delta_{singlet}$= 14.6 ppm, $C_1 = \ 9.83 \times 10^5$, $C_2 = 0\ (not\ optimized)$

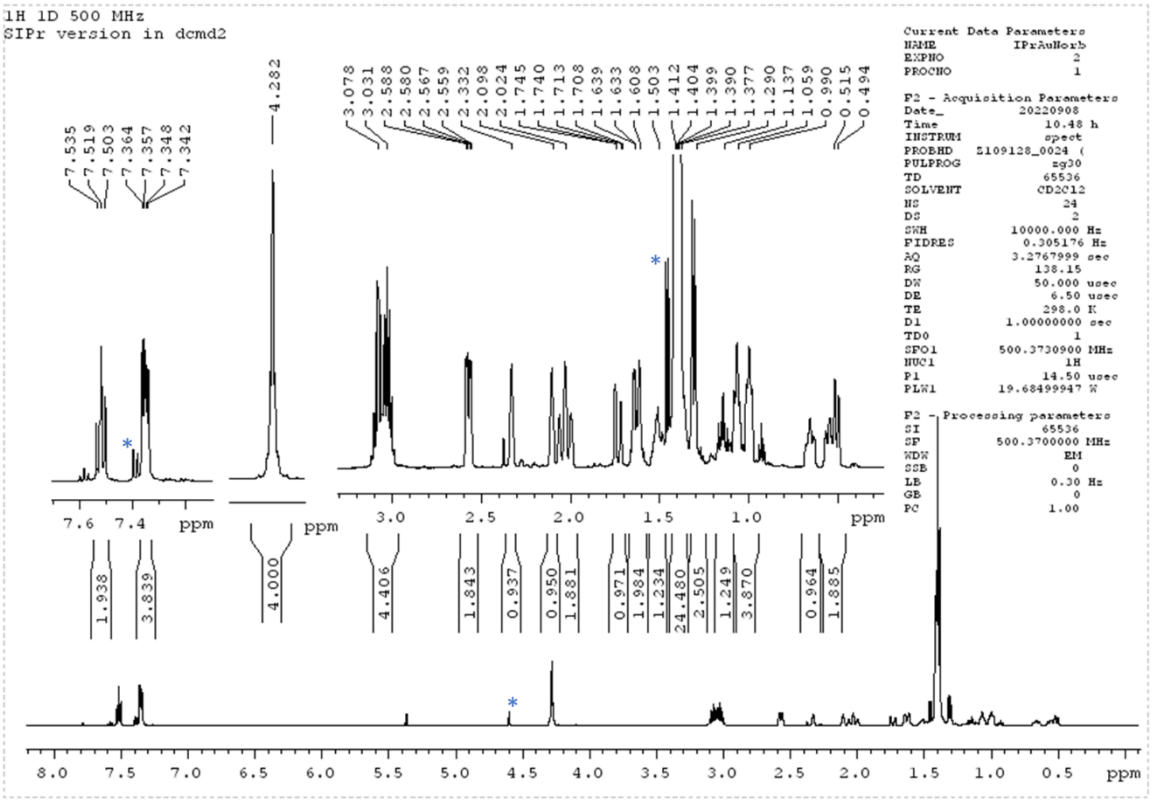

Figure S11. ^{1}H NMR spectrum of [(SIPr)Au(η^2-(Z) anti-(bis-2,2'-norbornylidene))]$^+$[SbF6]$^-$. *residual SIPr·HCl.

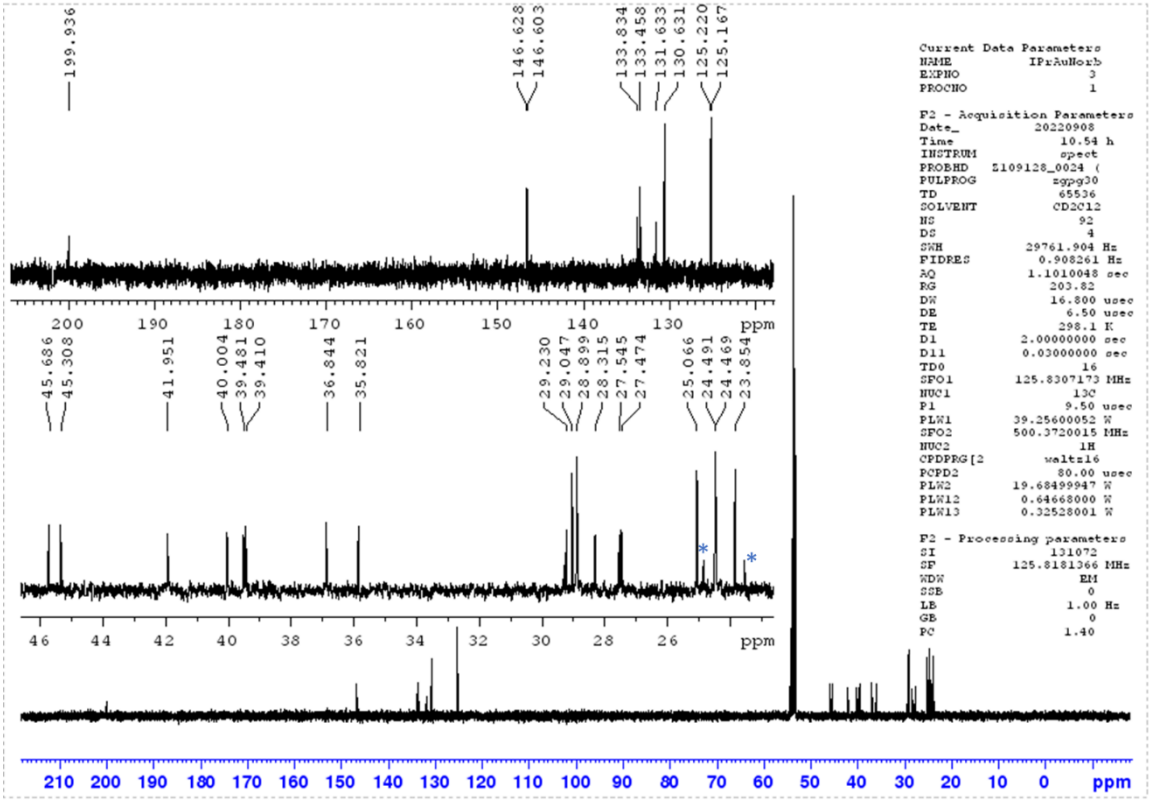

Figure S12. $^{13}C\{^{1}H\}$ NMR spectrum of [(SIPr)Au(η^2-(Z) anti-(bis-2,2'-norbornylidene))]$^{+}$[SbF6]$^{-}$. *residual SIPr·HCl.

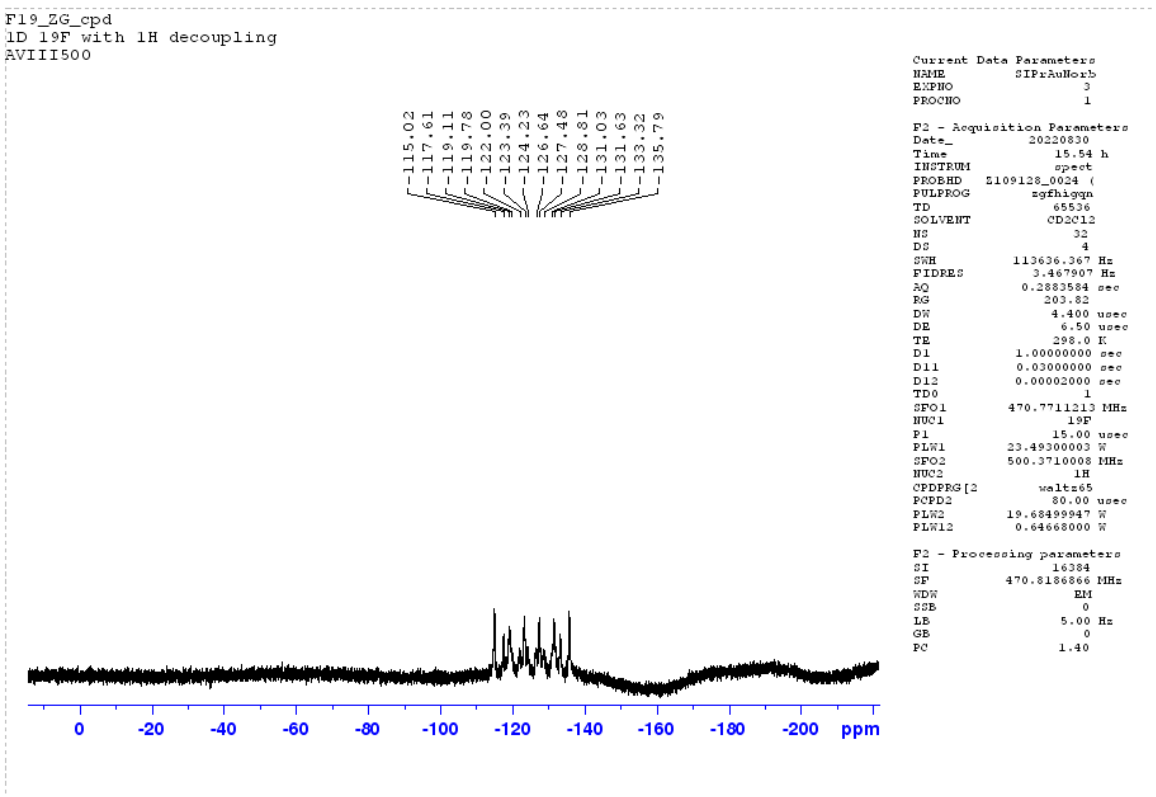

Figure S13. $^{19}F\{^{1}H\}$ NMR spectrum of [(SIPr)Au(η^2-(Z) anti-(bis-2,2'-norbornylidene))]$^+$[SbF6]$^-$.

Kinetic studies with varying [[Ni(^{i}Pr$_3$P)]$_5$H$_6$] with cyclooctene as hydrogen acceptor. Solution A was made by dissolving 40 mg of [Ni(^{i}Pr$_3$P)]$_5$H$_6$ in 800 mg of tBuOMe, solution B was made by dissolving 120mg of cyclooctene in 1000 mg of tBuOMe, solution C was made by dissolving 29 mg of ^{i}Pr$_3$P in 500 mg of tBuOMe. Approximate masses of 420mg, 210mg, 105mg, and 53mg of solution A, and 112 mg of solution B, and 53 mg of solution C were weighed in 4 NMR tubes and diluted to 600 mg of tBuOMe. HMDSO (0.02M) was used as internal standard in all samples. The NMR samples were kept in liquid nitrogen until the reaction could be monitored over time by 1H NMR spectroscopy at 298 K.

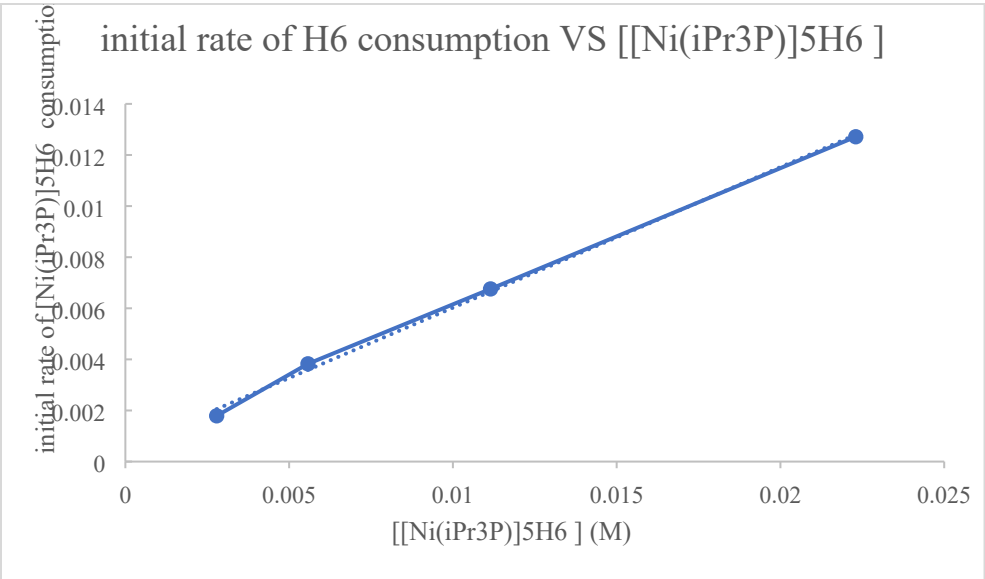

Figure S14. Influence of concentration of $[Ni(^{i}Pr_3P)]_5H_6$ on the rate of $[Ni(^{i}Pr_3P)]_5H_6$ consumption in the reaction with cyclooctene.

Kinetic studies with varying $[^{i}Pr_3P]$ with cyclooctene as hydrogen acceptor. 100 mg of $[Ni(^{i}Pr_3P)]_5H_6$ was dissolved in 2000 mg of tBuOMe as solution A, 120 mg of cyclooctene was dissolved in 1000 mg of tBuOMe as solution B, and 116 mg of $^{i}Pr_3P$ was dissolved in 200 mg of tBuOMe as solution C. To 4 NMR tubes each containing 420 mg of solution A were added 120 mg of solution B and solution C (126 mg, 63 mg, 32 mg, 16 mg, respectively). All samples were diluted to 600 mg of tBuOMe and contains HMDSO (0.02M) as internal standard. The NMR samples were kept in liquid nitrogen until the reaction could be monitored over time by 1H NMR spectroscopy at 298 K.

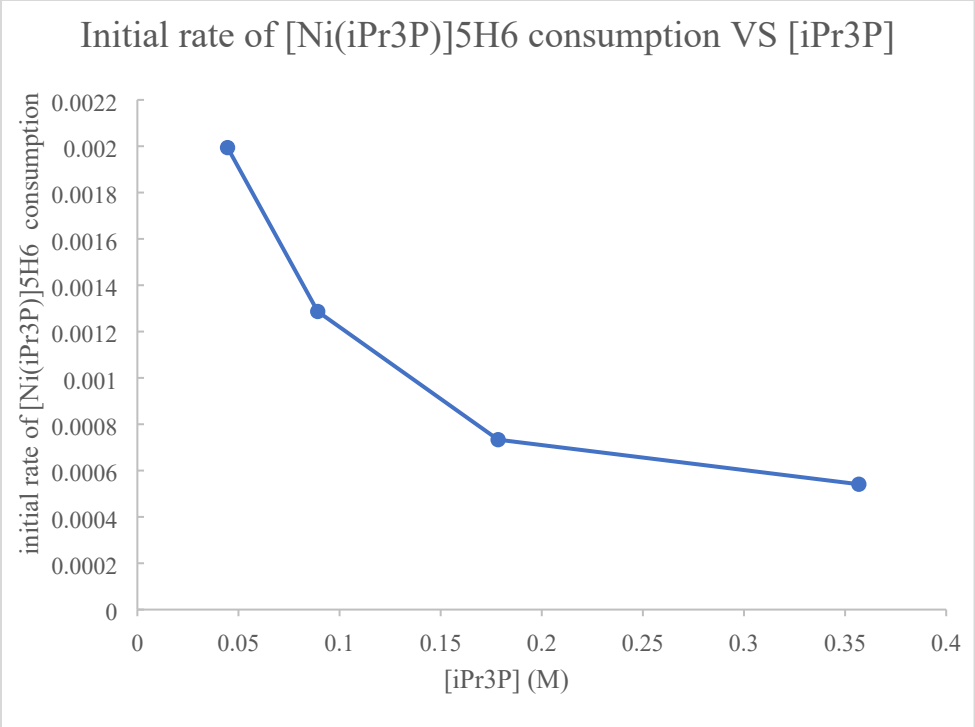

Figure S15. Influence of concentration of $^{i}Pr_3P$ on the rate of $[Ni(^{i}Pr_3P)]_5H_6$ consumption in the reaction with cyclooctene.

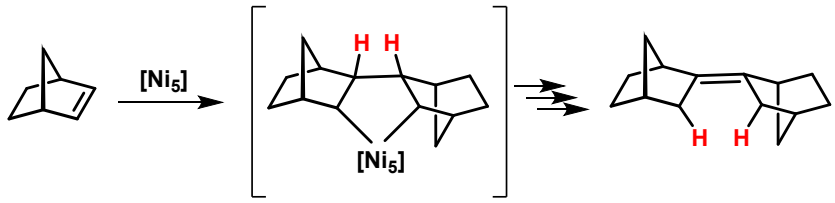

Scheme S2. Potential mechanism of coupling of norbornene through an oxidative addition step.

Synthesis of strained cyclic octyne 4, synthesized according to literature prep with modification.[13]

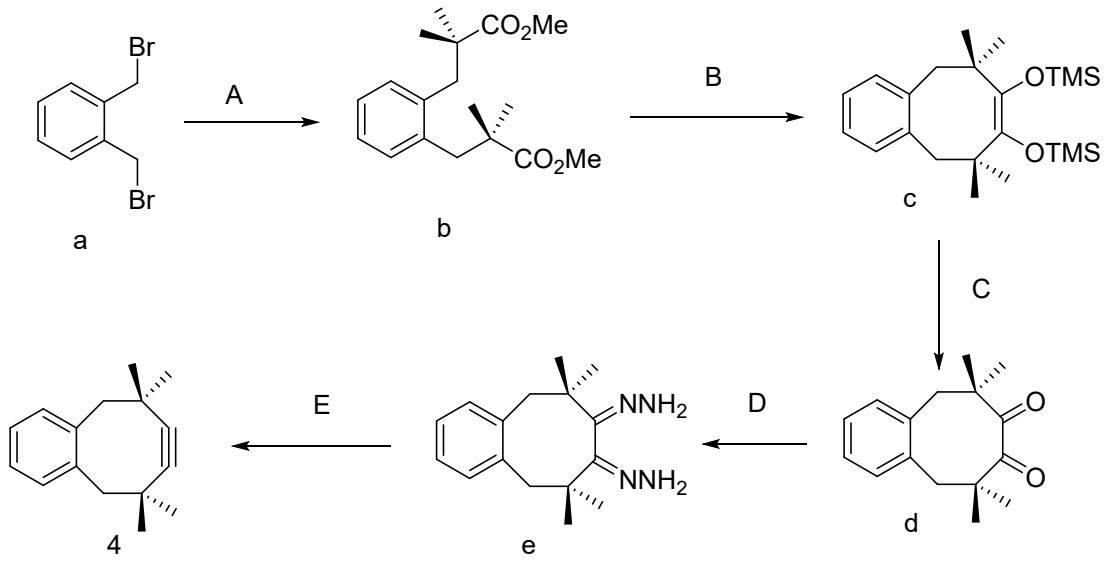

Step A, Synthesis of **b**.

To a THF solution of diisopropylamine (5 mL, 0.036 mol) at –78 °C, n-BuLi in hexane (2.0 M, 17.8 mL) was added dropwise, reaction mixture was stirred for 30 min and allowed warm to –40 °C, Methyl isobutyrate (4.1 mL, 0.036 mol) was added dropwise to the freshly made LDA solution. Reaction mixture then stirred for 30 min, and allowed to warm to room temperature. THF, hexane and diisopropylamine were removed under vacuum, as presence of diisopropylamine will decrease the yield of the reaction. Re-dissolve the methyl isobutyrate lithium salt in thf/n-pentane at room temperature and was cool to –40 °C, then add α,α′-Dibromo-o-xylene (4.5 g, 0.017 mol) in n-pentane dropwise at –40 °C, stir the reaction mixture overnight and covered with aluminum foil. Work up by quenching with cold DI water and extract with ethyl acetate. Dry organic layer with $MgSO_4$, then pump off solvent (4.96 g, 95%). Resulting ester **b** can also be recrystallized from chloroform. ^{1}H NMR (chloroform-d, 298 K, 500 MHz): δ 1.20 (s, 12H), 3.01 (s, 4H), 3.70 (s, 6H), 7.07 (m, 2H), 7.16 (m, 2H). ^{13}C{^{1}H} NMR (chloroform-d, 298 K, 125 MHz): δ 25.1 (s, 4C), 41.7 (s, 2C), 44.3 (s, 2C) , 51.8 (s, 2C) , 126.2 (s, 2C) , 130.7 (s, 2C) , 136.9 (s, 2C), 178.2 (s, 2C).

Step B: synthesis of **c**.

A 500 mL bomb, vacuum dried using a heat gun, and flushed with nitrogen three times was brought inside glovebox, filled with NaK (600 mg Na, 26.1 mmol), and 200 mL of toluene. A solution of b and Trimethylsilyl chloride (3.3 mL, 26.1 mmol) in 50 mL of toluene (2 g, 6.5 mmol) was added dropwise while heating to 50 °C. The reaction mixture was heated to 110 °C and stirred for 3 hrs, cooled and solvent was reduced under vacuum. The flask was brought inside the glove box, filtered through celite and washed with toluene. Then cyclic TMS ether c was obtained as a colourless oil and used in next step immediately without further purification. Yield: 2.06 g, 81 %. ^{1}H NMR (toluene-H_8, 298 K, 500 MHz): 0.089 (s, 18H), 1.33 (s, 12H), 2.75 (s, 4H), aromatic peaks overlap with toluene peaks.

Step C: Synthesis of **d**.

d Was synthesized by adapting a previously reported procedure for a similar substrate.[14] Dissolve **c** (2 g, 5.1 mmol) in 50 mL of DCM, then add a DCM solution of Br_2 (1.63 g, 10.2 mmol) dropwise to c at 0 °C, the orange color will disappear unless all **c** are consumed, and when the orange color persists, stir for a further 30 min to ensure complete reaction. Quench with water and sodium sulfite solution, extract the organic phase and dry with magnesium sulfate and remove all solvent under vacuum. The resulting diketone **d** can be recrystallized in hexane at –20 °C. ^{1}H NMR (chloroform-d, 298 K, 500 MHz): δ 1.23 (br s, 12H), 2.82 (br s, 4H), 7.10-7.19 (m, 4H, aromatic H). ^{13}C{^{1}H} NMR (chloroform-d, 298 K, 125 MHz): δ 23.7 (br s, 2C), 25.3 (br s, 2C), 43.8 (br s, 2C), 46.9 (s, 2C), 127.1 (s, 2C), 132.5 (s, 2C), 135.8 (s, 2C), 211.5 (s, 2C).

Step D: Synthesis of bis(hydrazone) **e**.

Heat **b** (500 mg, 2.06 mmol) with hydrazine monohydrate (614 mg, 12.3 mmol) and hydrazine monohydrochloride (674 mg, 12.3mmol) in 3 mL of ethylene glycol at 180 °C for 72 h in a sealed bomb. Cool to room temperature and work up by add diethyl ether, then filter through alumina column, then wash the column with diethyl ether to extract out dihydrazone, dry with $MgSO_4$ to give corresponding bis(hydrazone) **e** as slightly off-white solid (334 mg, 60 %). ^{1}H NMR (chloroform-d, 298 K, 500 MHz): δ 1.10 (s, 6H, Me), 1.30 (s, 6H, Me), 2.81 (s, 4H, benzylic), 5.17 (br s, 4H), 7.09-7.13 (m, 4H). ^{13}C{^{1}H} NMR (chloroform-d, 298 K, 125 MHz): δ 28.6 (2s, C), 29.3 (s, 2C), 42.4 (s, 2C), 46.1 (s, 2C), 126.3 (s, 2C), 131.8 (s, 2C), 137.8 (s, 2C), 152.4 (s, 2C).

Step E: Synthesis of the cyclic alkyne **4**.

Dissolve $Pb(OAc)_4$ in THF, and mix at –20 °C under N_2, then make a solution of bis(hydrazone) **e** in THF, and add to $Pb(OAc)_4$ dropwise and stir at –20 °C and gases evolve. Then let it warm up to room temperature and stir for 15 min in total. Filter through celite and pump dry under vacuum to remove acetic acid and THF, triturate with toluene and filter through silica plug to obtain a clear oil upon solvent removal under vacuum (81%). ^{1}H NMR (benzene-d_6, 298 K, 500 MHz): δ 0.99 (s, 6H), 1.17 (s, 6H), 2.31 (d, 2H, J=12.4 Hz), 3.41 (d, 2H, J=12.4 Hz), 6.97 (dd, 2H, J=3.4, 5.6 Hz), 7.11 (dd, 2H, J=3.4, 5.6 Hz). ^{13}C{^{1}H} NMR (benzene-d6, 298 K, 125 MHz): δ 24.9 (s, 2C), 29.4 (s, 2C), 34.0 (s, 2C), 52.9 (s, 2C), 101.5 (s, 2C), 126.2 (s, 2C), 133.8 (s, 2C), 139.4 (s, 2C).

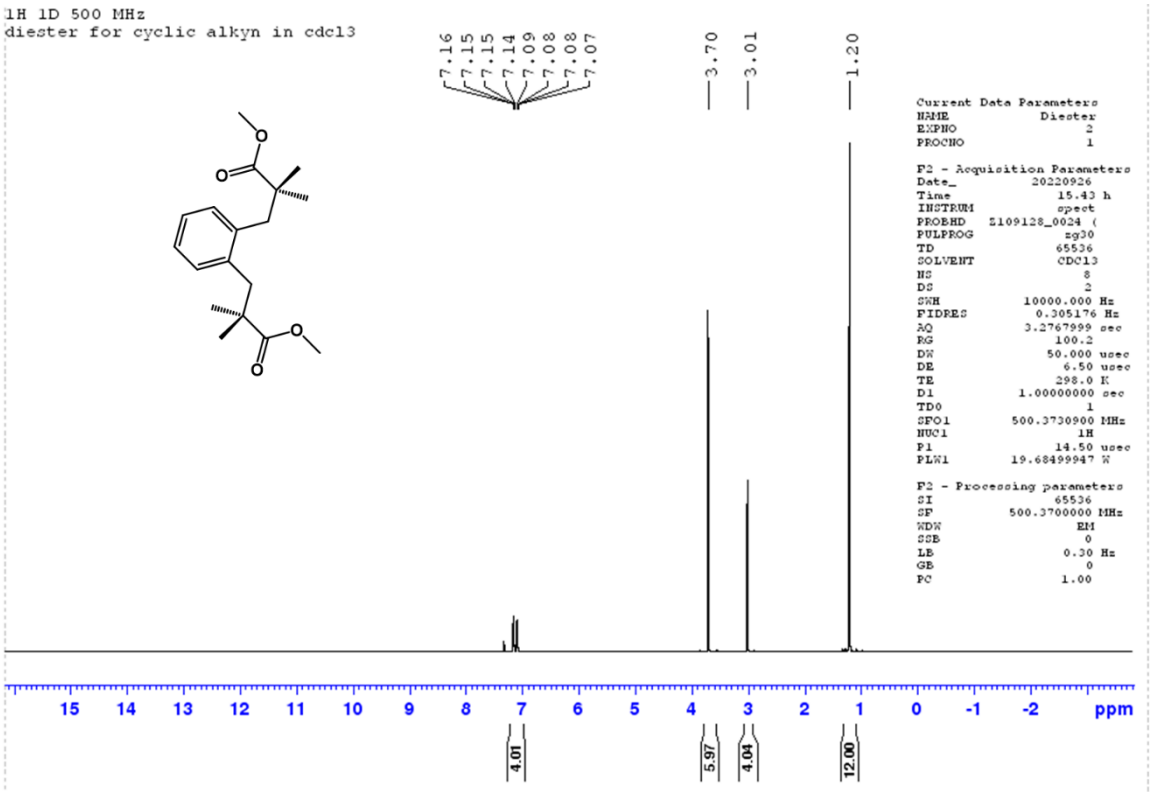

Figure S16. ^{1}H NMR spectrum of **b** in chloroform-d.

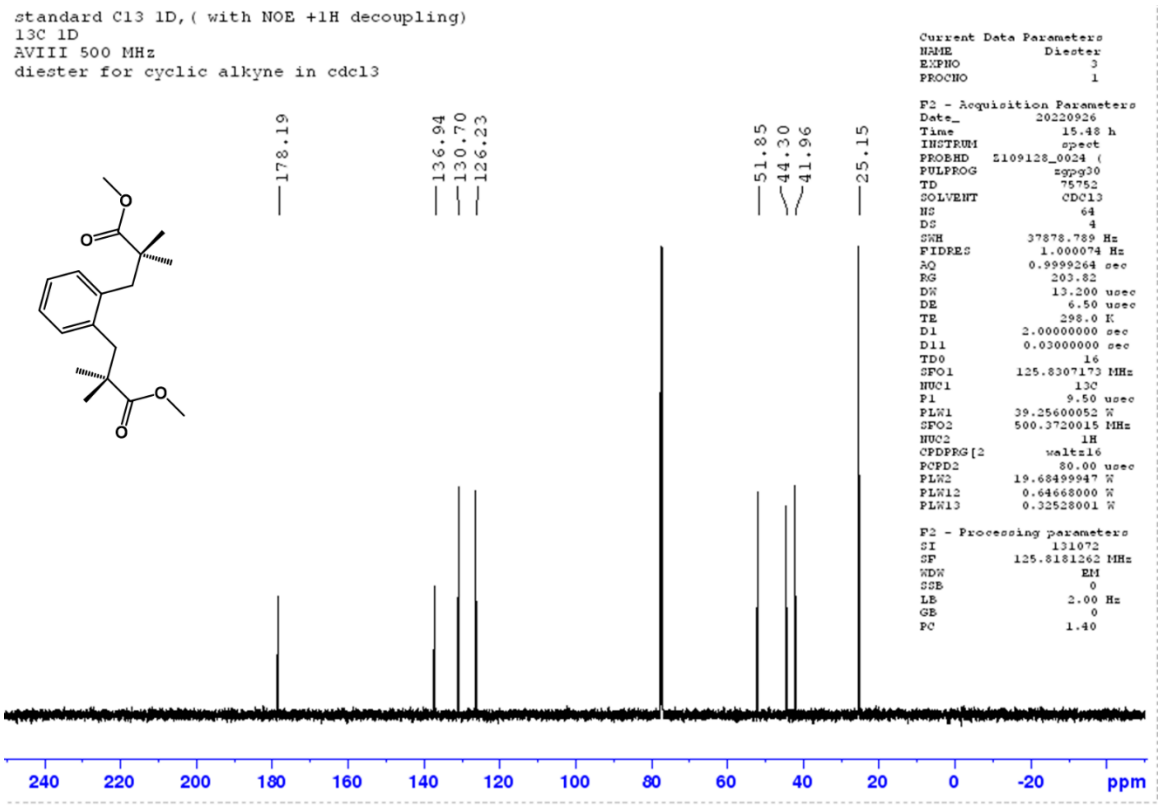

Figure S17 $^{13}C\{^{1}H\}$ NMR spectrum of **b** in chloroform-d.

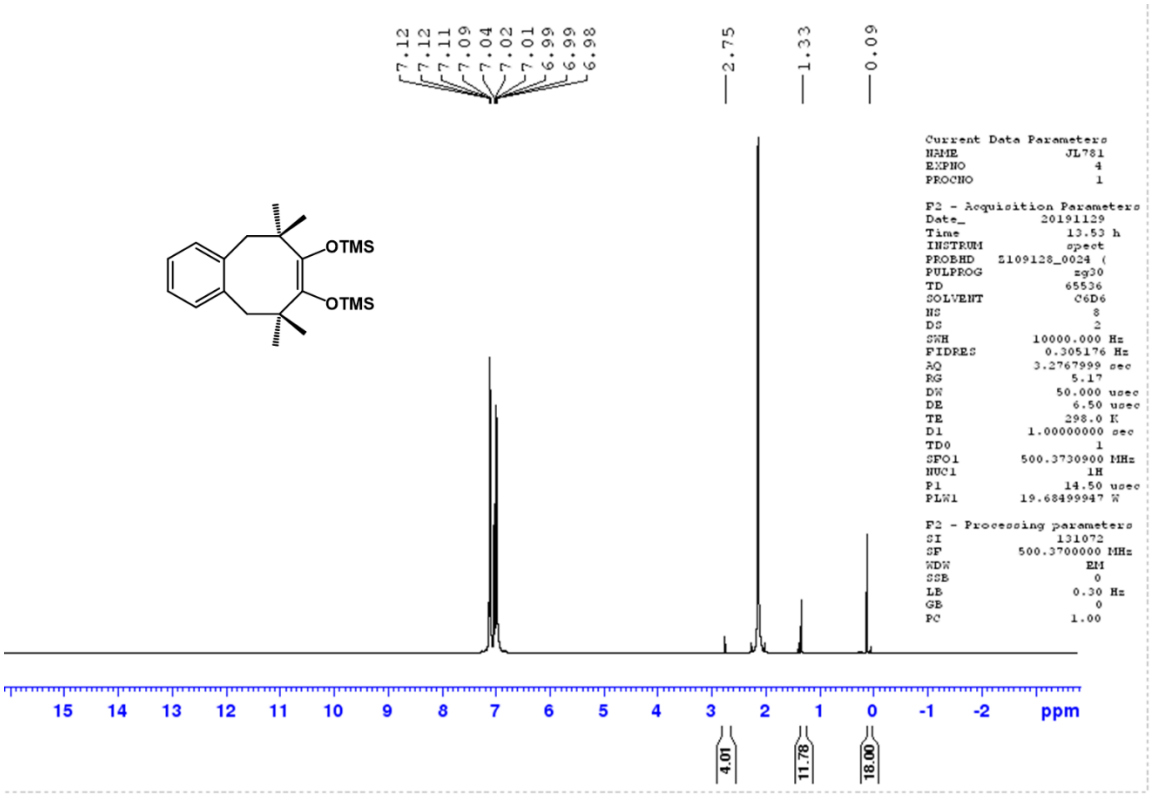

Figure S18. ^{1}H NMR spectrum of **c** in proteo-toluene.

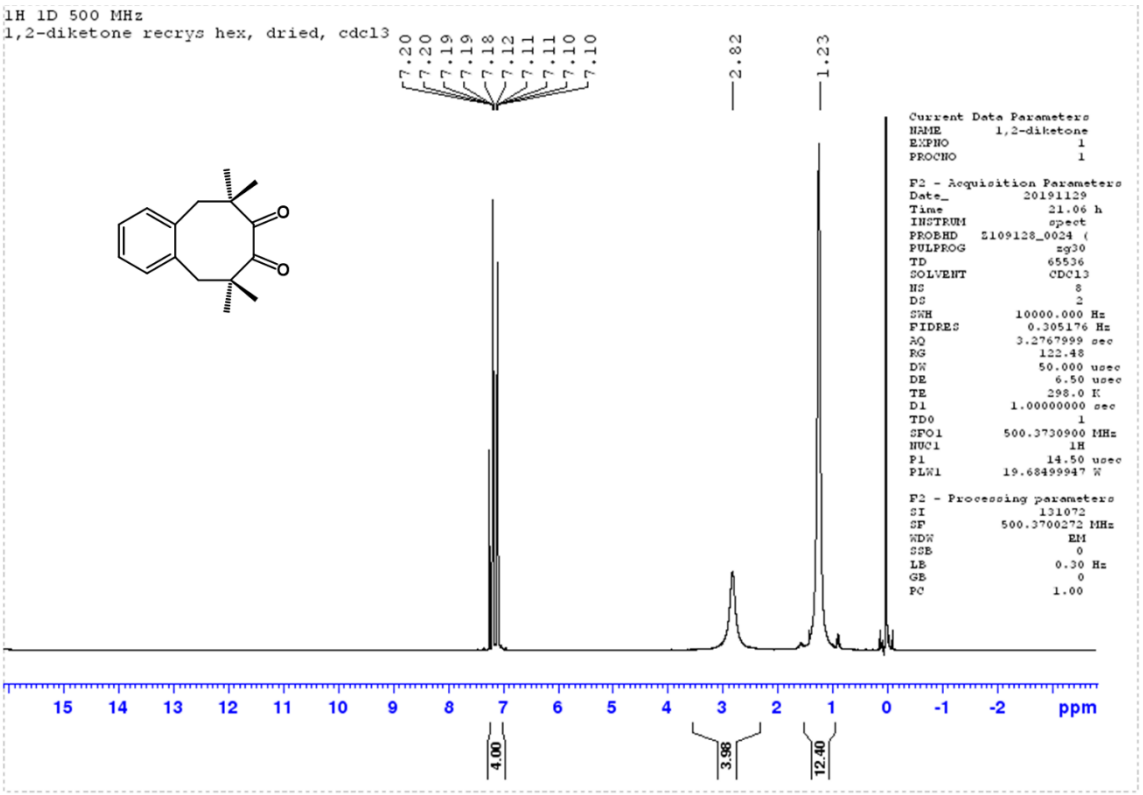

Figure S19. ^{1}H NMR spectrum of **d** in chloroform-d.

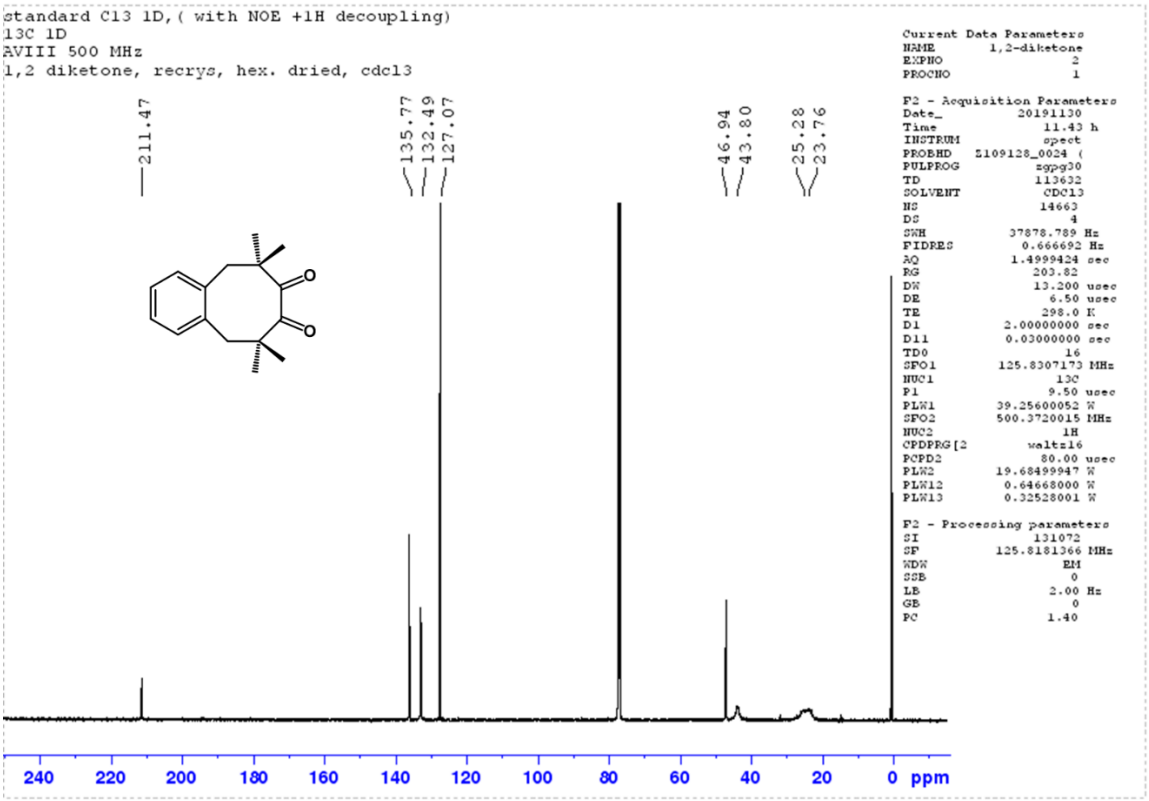

Figure S20. ^{13}C{^{1}H} NMR spectrum of **d** in chloroform-d.

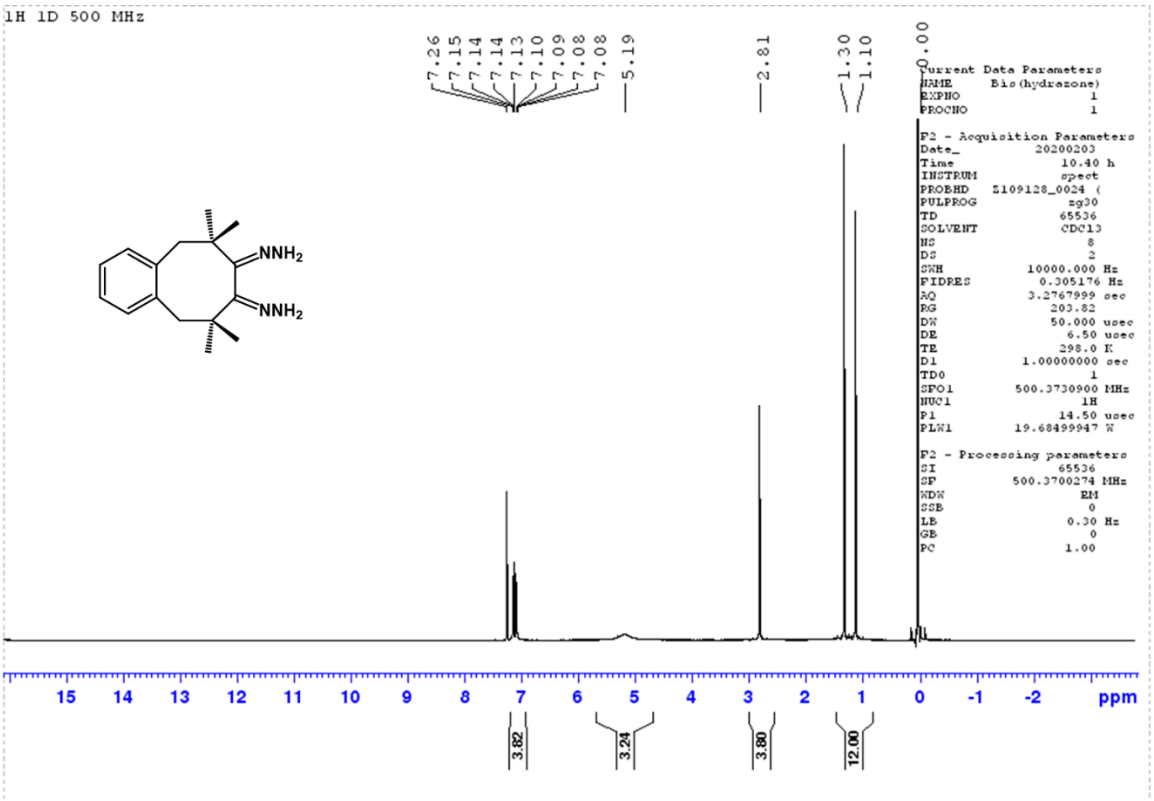

Figure S21. ^{1}H NMR spectrum of **e** in chloroform-d. $SiMe_4$ used as internal reference at δ 0.0

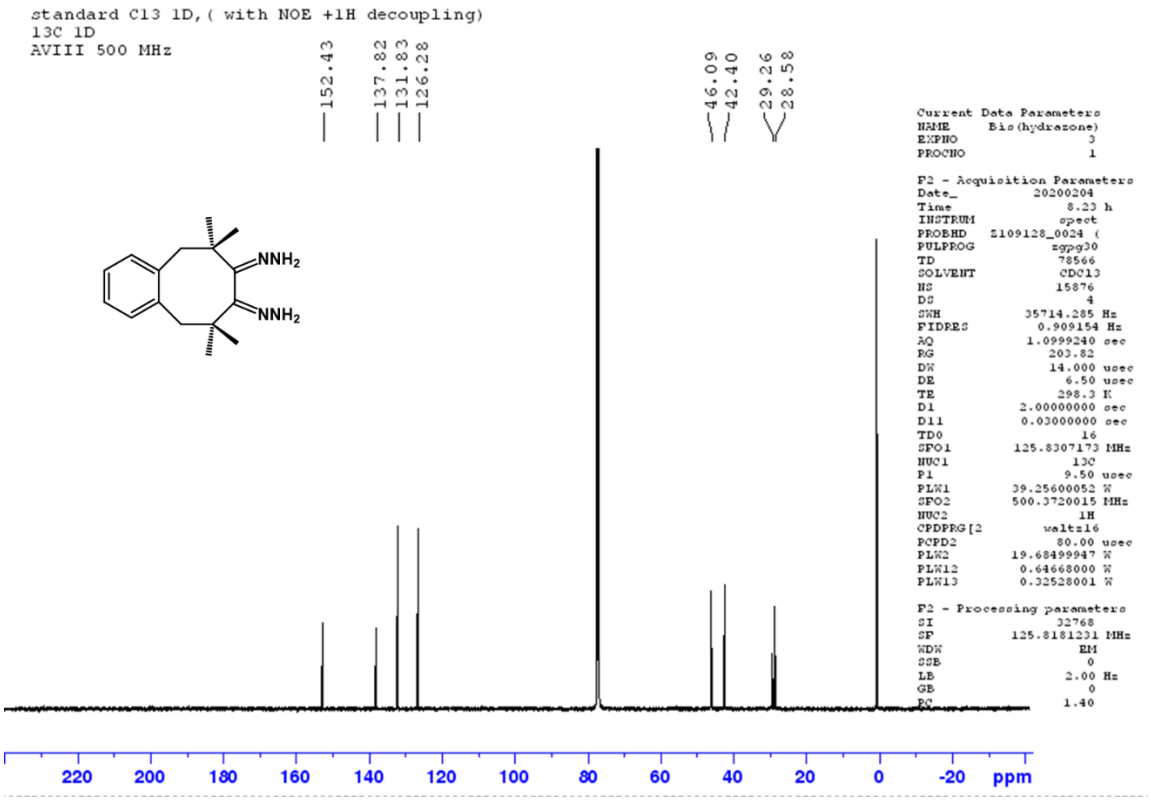

Figure S22. $^{13}C\{^{1}H\}$ NMR spectrum of **e** in chloroform-d. $SiMe_4$ used as internal reference at δ 0.0

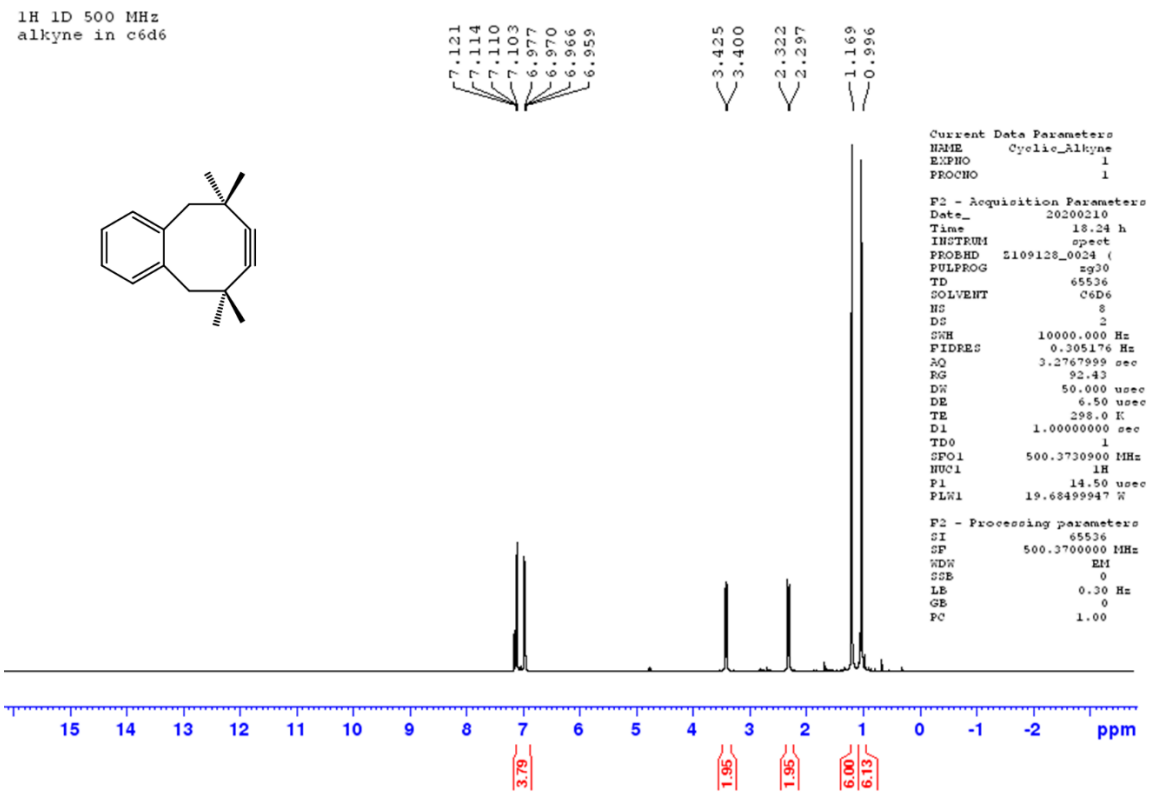

Figure S23. ^{1}H NMR spectrum of **4** in benzene-d_6.

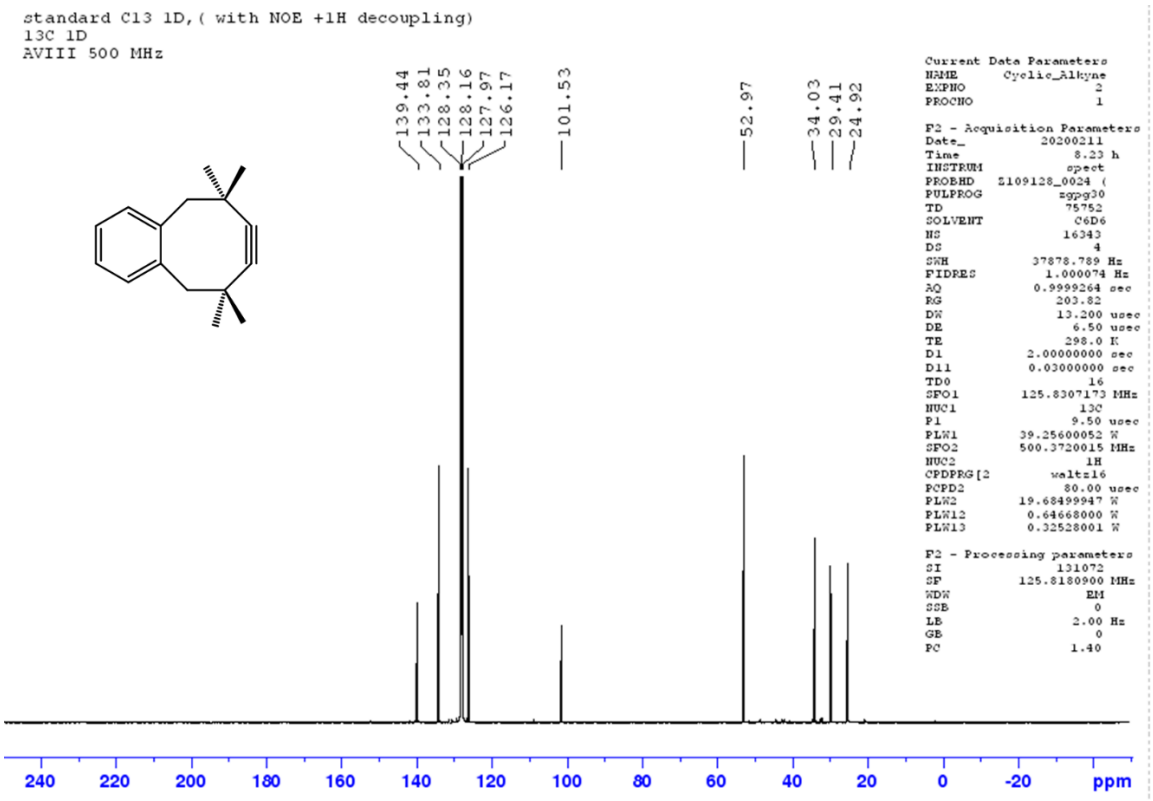

Figure S24. $^{13}C\{^{1}H\}$ NMR spectrum of **4** in benzene-d_6.

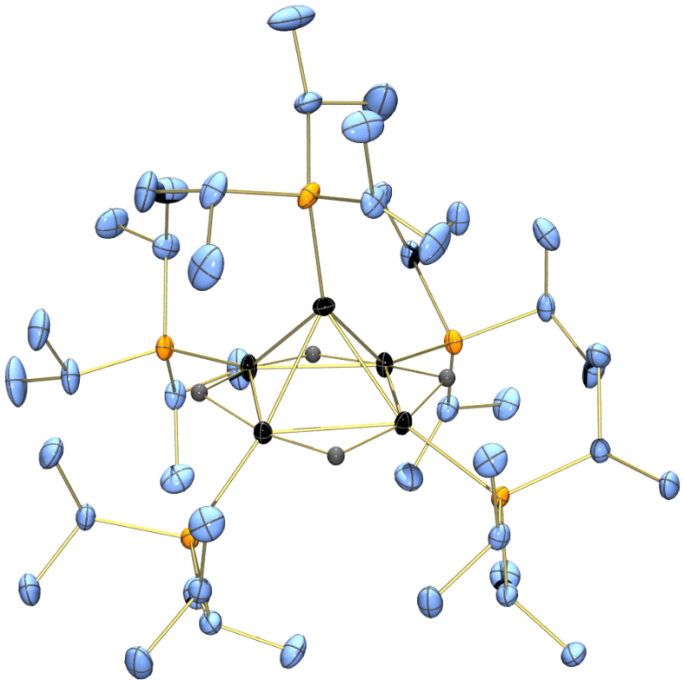

Crystallographic data and structure refinement of **3**

Empirical formula	$C_{45}H_{109}Ni_5P_5$
Formula weight	1098.72
Temperature/K	173(2)
Crystal system	triclinic
Space group	P-1
a/Å	12.4236(11)
b/Å	12.5504(11)
c/Å	20.9354(16)
α/°	93.244(3)
β/°	90.622(3)
γ/°	119.420(3)
Volume/Å^3	2836.0(4)
Z	2
ρ_{calc}g/cm^3	1.287
μ/mm^{-1}	1.797
F(000)	1188.0
Crystal size/mm^3	0.29 × 0.27 × 0.24
Radiation	MoKα (λ = 0.71073)
2Θ range for data collection/°	5.854 to 72.872
Index ranges	-20 ≤ h ≤ 20, -20 ≤ k ≤ 20, -34 ≤ l ≤ 34

Reflections collected	292412
Independent reflections	27574 [R_{int} = 0.0528, R_{sigma} = 0.0274]
Data/restraints/parameters	27574/63/576
Goodness-of-fit on F^2	1.074
Final R indexes [I>=2σ (I)]	R_1 = 0.0375, wR_2 = 0.0840
Final R indexes [all data]	R_1 = 0.0568, wR_2 = 0.0947
Largest diff. peak/hole / e $Å^{-3}$	2.05/-1.00

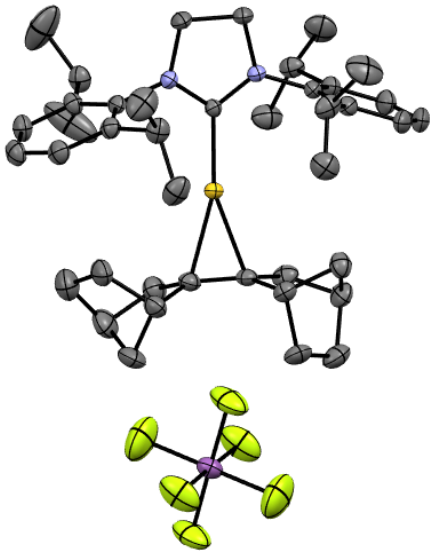

Crystallographic data and structure refinement of **[(SIPr)Au(η²-(Z) anti-(bis-2,2'-norbornylidene))]⁺[SbF6]⁻**

Empirical formula	$C_{41}H_{58}N_2F_6SbAu$
Formula weight	1011.61
Temperature/K	170(2)
Crystal system	monoclinic
Space group	Cc
a/Å	22.9956(14)
b/Å	10.0410(6)
c/Å	20.4012(12)
α/°	90
β/°	119.072(2)
γ/°	90
Volume/$Å^3$	4117.1(4)
Z	4
ρ_{calc}g/cm^3	1.632
μ/mm^{-1}	4.272
F(000)	2008.0

Crystal size/mm^3	0.06 × 0.06 × 0.05
Radiation	MoKα (λ = 0.71073)
2Θ range for data collection/°	4.054 to 72.494
Index ranges	-38 ≤ h ≤ 38, -16 ≤ k ≤ 16, -33 ≤ l ≤ 33
Reflections collected	104464
Independent reflections	19841 [R_{int} = 0.0710, R_{sigma} = 0.0464]
Data/restraints/parameters	19841/29/496
Goodness-of-fit on F^2	1.028
Final R indexes [I>=2σ (I)]	R_1 = 0.0319, wR_2 = 0.0687
Final R indexes [all data]	R_1 = 0.0392, wR_2 = 0.0724
Largest diff. peak/hole / e Å^{-3}	4.05/-0.84
Flack parameter	-0.004(2)

References:

1. R. Beck, M. Shoshani and S. A. Johnson, *Angew. Chem. Int. Ed.*, 2012, **51**, 11753-11756.
2. G. Capozzi, G. Romeo and F. Marcuzzi, *J. Chem. Soc. Chem. Comm.*, 1982, 959-960.
3. J. J. Eisch and J. N. Gitua, *Organometallics*, 2003, **22**, 24-26.
4. D. A. Roberts, B. S. Pilgrim, G. Sirvinskaite, T. K. Ronson and J. R. Nitschke, *J. Am. Chem. Soc.*, 2018, **140**, 9616-9623.
5. A. P. Marchand, D. Xing and S. G. Bott, *Tetrahedron*, 1996, **52**, 825-832.
6. P. d. Frémont, N. M. Scott, E. D. Stevens and S. P. Nolan, *Organometallics*, 2005, **24**, 2411-2418.
7. D. Janssen-Muller, B. Sahoo, S. Z. Sun and R. Martin, *Isr J Chem*, 2020, **60**, 195-206.
8. H. Sommer, F. Julia-Hernandez, R. Martin and I. Marek, *ACS Cent. Sci.*, 2018, **4**, 153-165.
9. V. M. Mohring and G. Fink, *Angew Chem Int Edit*, 1985, **24**, 1001-1003.
10. L. K. Johnson, C. M. Killian and M. Brookhart, *J. Am. Chem. Soc.*, 1995, **117**, 6414-6415.
11. H. Olivier-Bourbigou, P. A. R. Breuil, L. Magna, T. Michel, M. F. E. Pastor and D. Delcroix, *Chem. Rev.*, 2020, **120**, 7919-7983.
12. M. M. Shoshani, J. Y. Liu and S. A. Johnson, *Organometallics*, 2018, **37**, 116-126.
13. A. Krebs, J. Odenthal and H. Kimling, *Tetrahedron Letters*, 1975, **16**, 4663-4666.
14. F. W. Lewis, L. M. Harwood, M. J. Hudson, M. G. B. Drew, J. F. Desreux, G. Vidick, N. Bouslimani, G. Modolo, A. Wilden, M. Sypula, T.-H. Vu and J.-P. Simonin, *J. Am. Chem. Soc.*, 2011, **133**, 13093-13102.